1-31-2023

Columbia River Rhyolites: Age-Distribution Patterns and Their Implications for Arrival, Location, and Dispersion of Continental Flood Basalt Magmas in the Crust

Martin J. Streck
Portland State University, streckm@pdx.edu

Vanessa M. Swenton
Portland State University

William C. McIntosh
New Mexico Institute of Mining and Technology

Matt Heizler
New Mexico Institute of Mining and Technology

Citation Details

Streck, M.J.; Swenton, V.M.; McIntosh, W.; Ferns, M.L.; Heizler, M. Columbia River Rhyolites: Age-Distribution Patterns and Their Implications for Arrival, Location, and Dispersion of Continental Flood Basalt Magmas in the Crust. Geosciences 2023, 13, 46. https://doi.org/ 10.3390/geosciences13020046 geosciences

MDPI

Article

Columbia River Rhyolites: Age-Distribution Patterns and Their Implications for Arrival, Location, and Dispersion of Continental Flood Basalt Magmas in the Crust

Martin J. Streck [1,*], Vanessa M. Swenton [1], William McIntosh [2], Mark L. Ferns [3] and Matt Heizler [2]

[1] Department of Geology, Portland State University, Portland, OR 97207, USA
[2] NM Bureau of Geology, New Mexico Tech, Socorro, NM 87801, USA
[3] Science Department, Eastern Oregon University, La Grande, OR 97850, USA
* Correspondence: streckm@pdx.edu

Abstract: Columbia River province magmatism is now known to include abundant and widespread rhyolite centers even though the view that the earliest rhyolites erupted from the McDermitt Caldera and other nearby volcanic fields along the Oregon–Nevada state border has persisted. Our study covers little-studied or unknown rhyolite occurrences in eastern Oregon that show a much wider distribution of older centers. With our new data on distribution of rhyolite centers and ages along with literature data, we consider rhyolites spanning from 17.5 to 14.5 Ma of eastern Oregon, northern Nevada, and western Idaho to be a direct response to flood basalts of the Columbia River Basalt Group (CRBG) and collectively categorize them as Columbia River Rhyolites. The age distribution patterns of Columbia River Rhyolites have implications for the arrival, location, and dispersion of flood basalt magmas in the crust. We consider the period from 17.5 to 16.4 Ma to be the waxing phase of rhyolite activity and the period from 15.3 to 14.5 Ma to be the waning phase. The largest number of centers was active between 16.3–15.4 Ma. The existence of crustal CRBG magma reservoirs beneath rhyolites seems inevitable, and hence, rhyolites suggest the following. The locations of centers of the waxing phase imply the arrival of CRBG magmas across the distribution area of rhyolites and are thought to correspond to the thermal pulses of arriving Picture Gorge Basalt and Picture-Gorge-Basalt-like magmas of the Imnaha Basalt in the north and to those of Steens Basalt magmas in the south. The earlier main rhyolite activity phase corresponds with Grande Ronde Basalt and evolved Picture Gorge Basalt and Steens Basalt. The later main phase rhyolite activity slightly postdated these basalts but is contemporaneous with icelanditic magmas that evolved from flood basalts. Similarly, centers of the waning phase span the area distribution of earlier phases and are similarly contemporaneous with icelanditic magmas and with other local basalts. These data have a number of implications for long-held notions about flood basalt migration through time and the age-progressive Snake River Plain Yellowstone rhyolite trend. There is no age progression in rhyolite activity from south-to-north, and this places doubt on the postulated south-to-north progression in basalt activity, at least for main-phase CRBG lavas. Furthermore, we suggest that age-progressive rhyolite activity of the Snake River Plain–Yellowstone trend starts at ~12 Ma with activity at the Bruneau Jarbidge center, and early centers along the Oregon–Nevada border, such as McDermitt, belong to the early to main phase rhyolites identified here.

Keywords: Columbia River Rhyolites; Columbia River Basalt; eastern Oregon; rhyolite flare-up; continental flood basalt

Citation: Streck, M.J.; Swenton, V.M.; McIntosh, W.; Ferns, M.L.; Heizler, M. Columbia River Rhyolites: Age-Distribution Patterns and Their Implications for Arrival, Location, and Dispersion of Continental Flood Basalt Magmas in the Crust. *Geosciences* **2023**, *13*, 46. https://doi.org/10.3390/geosciences13020046

Academic Editors: Ciro Cucciniello and Jesus Martinez-Frias

Received: 7 January 2023
Accepted: 23 January 2023
Published: 31 January 2023

1. Introduction

Lavas of the Columbia River Basalt Group (CRBG) of the Pacific Northwest of the United States (Figure 1) are of one of the most extensively studied flood basalts on our planet, and they serve as an archetypal example of vast outpourings of mafic lavas associated with the arrival of mantle plumes (e.g., [1,2]). There is no other flood basalt province with the level of knowledge on stratigraphy, eruption sites, and petrogenesis that we have for the CRBG, which has been established by many workers over several decades (e.g., [3–11]; and other papers in GSA spec pap 497, 2013). The traditional view of the CRBG was that flood basalts are not associated with abundant contemporaneous rhyolites, and the first rhyolites of note were those closely tied to the plume head-to-tail transition at the McDermitt volcanic field (Figure 1) (e.g., [5]). This interpretation since evolved for several reasons, an example of which being that more age determinations have reduced the temporal offset of CRBG lavas [3,12], thus bringing them closer in age to the mid-Miocene rhyolites of the province that were known for decades e.g., [13,14]. It is now clear that basaltic lavas of the CRBG are associated with contemporaneous rhyolites that erupted across the province from ~17.0 to ~14.5 Ma [7–9,15–19].

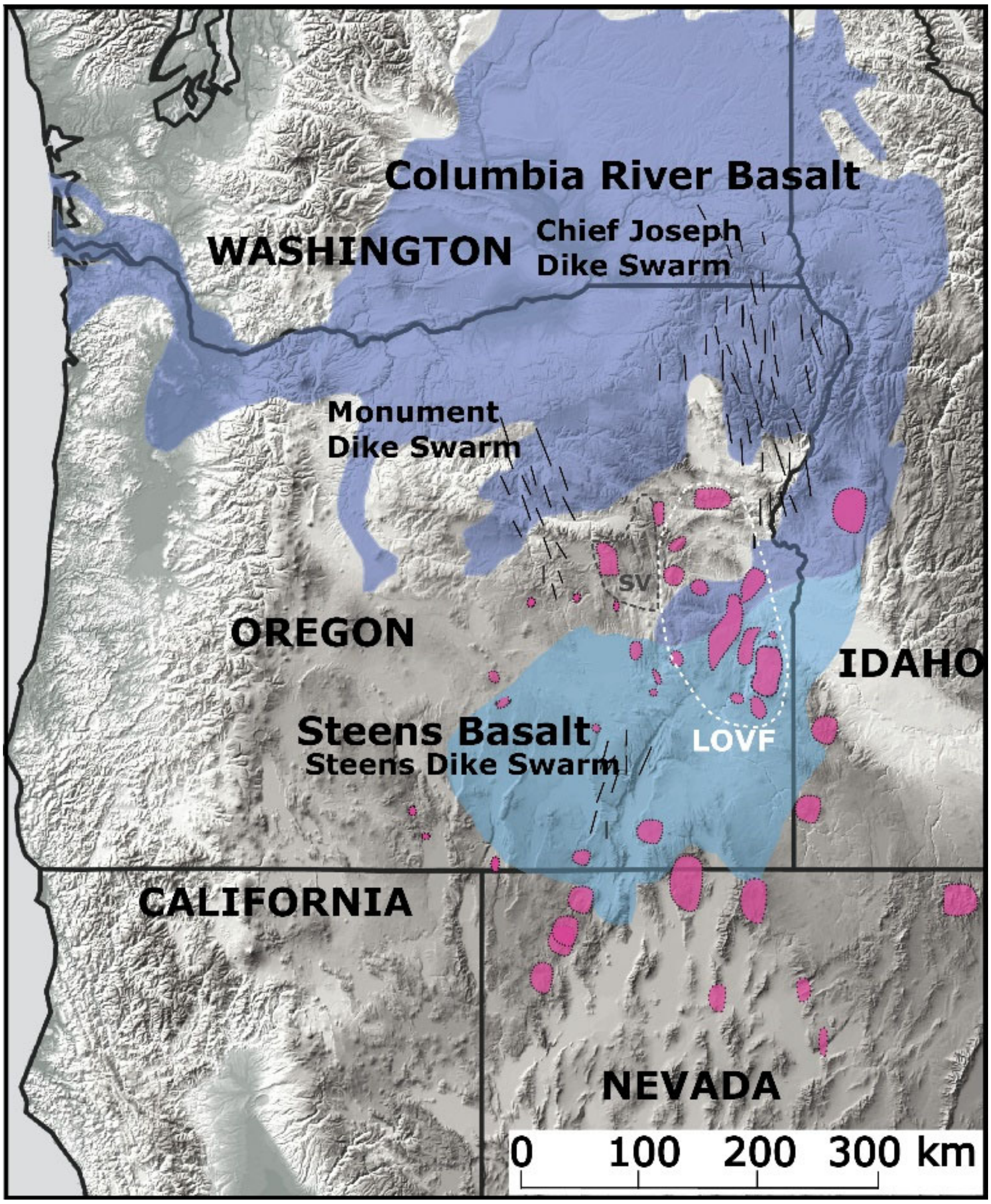

Figure 1. Regional setting of flood basalt lavas (blue) of Columbia River Basalt Group (CRBG) in the Pacific Northwest of the United States along with location of the three main dike swarms and 17.5–14.5 Ma rhyolite centers (red) discussed in this paper. White dashed line delimits the current extent of the Lake Owyhee volcanic field (LOVF) (cf. [7]); gray dashed line represents the extent of the Strawberry Volcanics (SV).

As consequence of this development, the Columbia River Basalt province has become recognized as a strongly bimodal (basalt–rhyolite) large igneous province (LIP) (Figure 1) ([7]), similar to what appears to be the typical case for continental flood basalt provinces elsewhere [20,21]. However, while a wealth of data has been published for rhyolites along the southern margin of the Oregon/Nevada/Idaho border [15,17,22–26], rhyolites farther north in Oregon lacked particularly important age and stratigraphic data, and the existence of some was virtually unknown. Therefore, current relationships of the mafic to silicic component of the Columbia River LIP are based on an incomplete and possibly biased data set. Furthermore, rhyolites offer important additional aspects on the dynamics of the Columbia River Basalt province and on continental LIPs. Dating rhyolites provides valuable information because age determinations of the basalts can be problematic and because precision can be insufficient for resolving timing issues (cf. [3,12,27]). Gathering data on rhyolite exposures, eruptive centers, and their storage sites is critical because fissure eruption sites of basalts may be displaced far from where basalt magmas were initially stored in crustal magmatic reservoirs or delivered from the mantle due to efficient lateral transport in dikes and sills (e.g., [28,29]). Hence, rhyolites can serve as critical stratigraphic markers, yielding high-precision ages, and rhyolites are clear indicators of where thermal pulses originating from the mantle are delivered to the crust via injection of basalt irrespective of the details of rhyolite petrogenesis (e.g., [30]). Consequently, rhyolites offer an alternative and complementary perspective on the temporal evolution of the arrival, dispersion, and storage of flood basalt magmas. In turn, this has implications for the causes of flood basalt magmatism and on whether these magmas are indeed generated due to the arrival of a mantle plume or rather mark other tectonic events (e.g., [31–34]).

We have investigated the timing, distribution, and composition of all rhyolites of the Lake Owyhee volcanic field (LOVF) and rhyolites farther north and west (Figure 1). Here, we present our current results and, in doing so, focus on rhyolites that fall into the time window of main stage CRBG activity. We recently reported on ages of late-to-mid-Miocene rhyolites within our study area in eastern Oregon that focused on the relationships of rhyolites associated with flood basalt magmatism and on rhyolites that are younger and are part of the High Lava Plain trend [34]; the main aspects of the compositional data of the rhyolites will be addressed elsewhere. We combine our data with data from the literature to discuss a province-wide view of rhyolite volcanism of the Columbia River magmatic province. Rhyolites of this study have not received the same attention as rhyolites along the Oregon-Nevada border (Figures 1 and 2), and much of what is known about the timing of these units goes back to data compiled 40 years ago [13]. Adding to the importance of these rhyolites is that the rhyolites of the LOVF (Figure 1) [7,18] are nearly co-spatial with the presumed topographic uplift associated with the thermal anomaly of the Columbia River Basalt province [35]—as well as with the convergence zone of CRBG dikes, aeromagnetic anomalies, and other large-scale features (Figure 2D) [36]—which led to speculation of crustal reservoirs of CRBG magmas in this area [11].

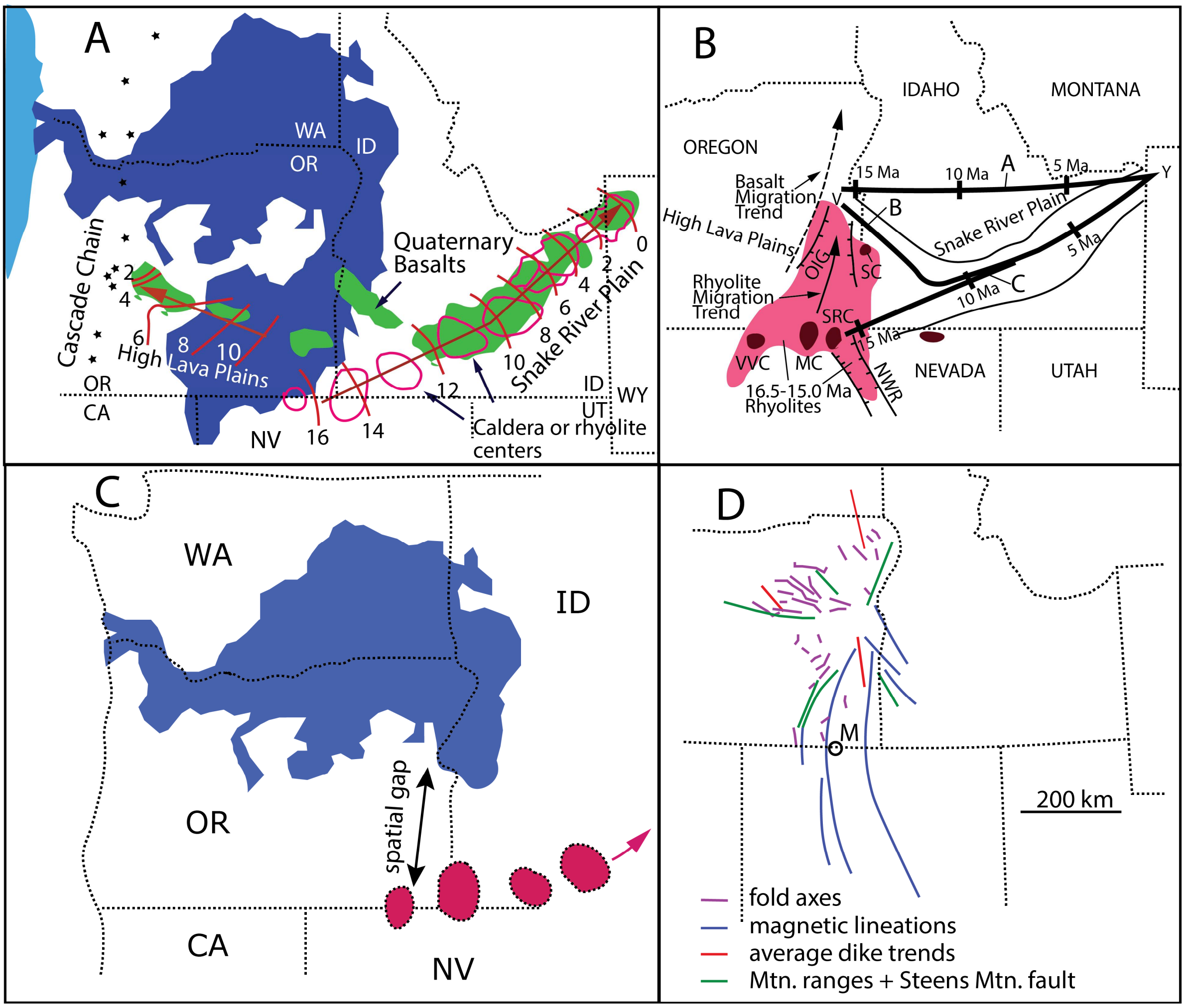

Figure 2. (**A**) Traditional representation of age-progressive rhyolites and rhyolite caldera centers of the Pacific Northwest, marked by age isochrones in Ma and arrows (red) in relation to flood basalts (blue), and stars mark location of large Cascade volcanoes (redrawn from [5]). (**B**) After [37], highlighting apparent migration trends within CRBG lavas and 16.5–15.0 Ma rhyolites that are deduced from age data prior this study in relation to the two discussed mantle impingement areas near McDermitt Caldera (MC) and near the town of Vale (V). Dark red ovals mark presumed oldest center, Virgin Valley Caldera (VVC), Santa Rosa-Calico (SRC), and Silver City (SC); other abbreviations: Yellowstone (Y), Oregon Idaho Graben (OIG), Northwestern Nevada Rift (NWR); A, B, C denote possible migration trends of the Yellowstone hotspot discussed in [37]; (**C**) Figure depicting spatial gap between first recognized rhyolite centers and Columbia River Basalt prior to incorporating the Steens Basalt, redrawn from [37]; (**D**) Pacific Northwest, showing large-scale physiographic, geologic, and geophysical features converging north of the McDermitt volcanic center, which is labeled "M" (figure redrawn from [36]).

Historical Perspective on Rhyolites of the Columbia River Province

The classical view of relating mid-Miocene rhyolites of the tri-state area of Oregon, Nevada, and Idaho to the massive outpouring of the flood basalts of the Columbia River Basalt involves a mantle plume impinging along the Oregon–Idaho border, initially causing flood basalt eruptions and generating rhyolites of the McDermitt volcanic field shortly thereafter (Figure 2C) (e.g., [38]). Rhyolite generation at the McDermitt volcanic field was tied to the beginning of the tail stage of the mantle plume that moved progressively northeastward from 16.5 Ma onward to create the Snake River Plain age-progressive rhyolite trend, culminating at present-day Yellowstone National Park (Figure 2A). This view later incorporated the northwest migrating silicic volcanism of the High Lava Plains as some complication to the Snake River Plain trend (Figure 2A) [39,40]. Since the mantle plume hypothesis was formulated to explain Columbia River Basalt and Snake River Plain rhyolites, skeptics of this hypothesis have pointed to the spatial offset between eruption sites of Columbia River Basalt (CRB) lavas and the initiation of the rhyolite trend (Figure 1) (e.g., [41]), as well as the aforementioned complications, to explain the two mirrored trends of regional silicic volcanism. Instead, researchers have argued for a tectonic cause for flood basalts and rhyolites (e.g., [42]). Furthermore, there are also compositional aspects of the CRBG that question a deep mantle origin.

Incorporation of the Steens Basalt as part of the same event as CRB flood basalts in the early 2000s (Figure 1) (e.g., [8,16]) and establishment what is now known as the Columbia River Basalt Group (CRBG) significantly extended the area from which basalts related to the supposed plume head stage erupted. This reduced the spatial discrepancy between eruption sites of earlier flood basalts to subsequent tail related rhyolites. Although silicic centers from farther north with similar ages to McDermitt have been known since 1975 [13,14,40,43,44], it was not until the early 2000s that attention was paid to mid-Miocene rhyolite occurrences outside of the McDermitt area. The works of [8,16,18], were instrumental in shining a spotlight on 15 Ma rhyolites from areas in Oregon that are north of McDermitt, particularly around the LOVF. Newer mapping [15,17,22,23,27,45,46] extended the area of rhyolites with ages similar to the 16.5 Ma McDermitt rhyolites to a broader region spanning from NW Nevada to McDermitt to the tri-state border of Oregon, Nevada, and Idaho. Given the extended footprint of basaltic eruptions and cogenetic, mid-Miocene rhyolites, the question of where the possible mantle plume impinged has become a moving target. For some, the general view of hotspot inception around McDermitt has prevailed (e.g., [47,48]), while other researchers are beginning to recognize the importance of the northward-trending swath of mid-Miocene rhyolites in Oregon [9,17,35,49]. This discussion is also fueled by other data that point to a more northern impingement of the plume head (or mantle upwelling in general), such as paleodrainage patterns suggesting a mid-Miocene topographic high and aeromagnetic maps showing lineaments converging farther north (Figure 2D) (e.g., [35,36] and references therein). The convergence of aeromagnetic lineaments and the orientations of dikes led Wolff et al. [11] to suggest that all CRBG magmas were stored in a common area in the crust coinciding with this convergence zone before traveling in dikes to their respective eventual eruption sites. Despite these data, older ages of rhyolites around the McDermitt caldera are viewed as a key argument in favor of a plume impingement location near McDermitt rather than farther north around the town of Vale (Figure 1) [37].

Most recently, however, the plume hypothesis to explain CRBG lavas has been questioned again, and the CRBG has been related to a growing tear in the downgoing slab of the subducted lithosphere [33]. Their study has placed renewed emphasis on the northward age progression of basalt eruption sites from the Steens Basalt dike swarm in the south to the later Chief Joseph dike swarm in the north, which is supposedly mirrored by the trend of silicic volcanism from McDermitt to rhyolites farther north (Figure 1) [37]. Finally, there are now models that have related the CRBG flood basalt province to the older, Eocene coastal flood basalt province of Siletzia within Oregon and Washington [50,51] and other models [52].

From the discussion above, it is clear that the debate on the origin of the CRBG is ongoing and that rhyolites are an important component that may prove critical in understanding the waxing and waning of volcanism of this continental LIP, thereby contributing to a broader understanding of the development of continental bimodal flood basalt provinces. Our study closes an existing data gap. The new data may not resolve the plume-versus-non-plume models for the CRBG, but they certainly help generate a more accurate understanding of the silicic component of the province that is currently incomplete and somewhat skewed.

2. Methods

Over the last 12 years, fieldwork by numerous Portland State University graduate students was conducted to collect samples in order to map stratigraphic sections or to map whole rhyolite occurrences where no previous map existed. Samples were collected from representative outcrops across the study area. Major and trace element geochemical data, phenocryst data, and lithological characteristics were used to distinguish units. Samples of silicic units within the study region that were known to be undated or imprecisely dated were selected for dating.

Major and trace element compositions of samples were determined using X-ray fluorescence spectroscopy (XRF) and inductively coupled plasma mass spectrometry (ICP-MS) at the Geoanalytical Lab at Washington State University (WSU). Sample preparation followed standard procedures of the lab [8,53].

Samples with fresh feldspar phenocrysts were the primary targets for $^{40}Ar/^{39}Ar$ dating. Thin sections were prepared by Spectrum Petrographics in Vancouver, Washington. Thin sections from one or two samples of each eruptive center were petrographically analyzed to determine which had suitable feldspars and to identify the best candidates for $^{40}Ar/^{39}Ar$ analysis. A series of mineral separation techniques were implemented to isolate clean feldspar phenocrysts from each sample, including but not limited to magnetic separation, HF acid leaching, and heavy liquid separation. Groundmass fractions were similarly cleaned, separated, and analyzed if feldspar phenocrysts were too altered or too sparse for analysis. Single-crystal total fusion was the preferred method for dating feldspar phenocrysts, and incremental heating was preferred for groundmass. Supplementary Materials contain information regarding procedures and analytical methods for $^{40}Ar/^{39}Ar$ analysis, and it also notes the institution at which each sample was analyzed.

3. Results

3.1. Mid Miocene Rhyolite Centers in Eastern Oregon

Below, we present a synopsis of our work on numerous mid-Miocene centers of rhyolite volcanism in eastern Oregon (Figure 3). Our acquired data consist of field work revealing distribution and stratigraphic information, bulk rock and mineral compositional data, and select radiometric ages from Ar–Ar geochronology.

3.1.1. Dooley Mountain Rhyolite Field

The Dooley Mountain rhyolite field (location number 1 on Figure 4) is the northernmost mid-Miocene rhyolite center, and it is considered part of the Lake Owyhee volcanic field of [43]. The Lake Owyhee volcanic field (LOVF) is a ~300 km long north–south belt of volcanic vents extending from Dooley Mountain on the north through the Oregon–Idaho graben to the McDermitt volcanic field on the south [7]; however, in recent years, the McDermitt volcanic field has been treated separately (e.g., [17]). First referred to as the Dooley Mountain rhyolite breccia, the rhyolite eruptive center at Dooley Mountain is a strongly eroded series of overlapping domes, lava flows, and likely subvolcanic intrusions that are bordered by marginal debris flow and block-and-ash-flow deposits. The complex also includes several small, locally sourced ash-flow tuffs and fallout tuffs [54]. Rhyolite domes are locally faulted and are extensively altered in some places.

Many units are locally intruded by glassy rhyolite and pyroclastic dikes (Figure 5). Rhyolite lava flows on the north and south flanks of Dooley Mountain overlie unit 2 of the Dinner Creek Tuff (cf. [19]). Erosional remnants of both proximal and distal facies of rhyolitic debris-flow and block-and-ash-flow deposits originating from Dooley Mountain also overlie the Dinner Creek Tuff in the Cenozoic sedimentary section exposed to the northeast of Dooley Mountain.

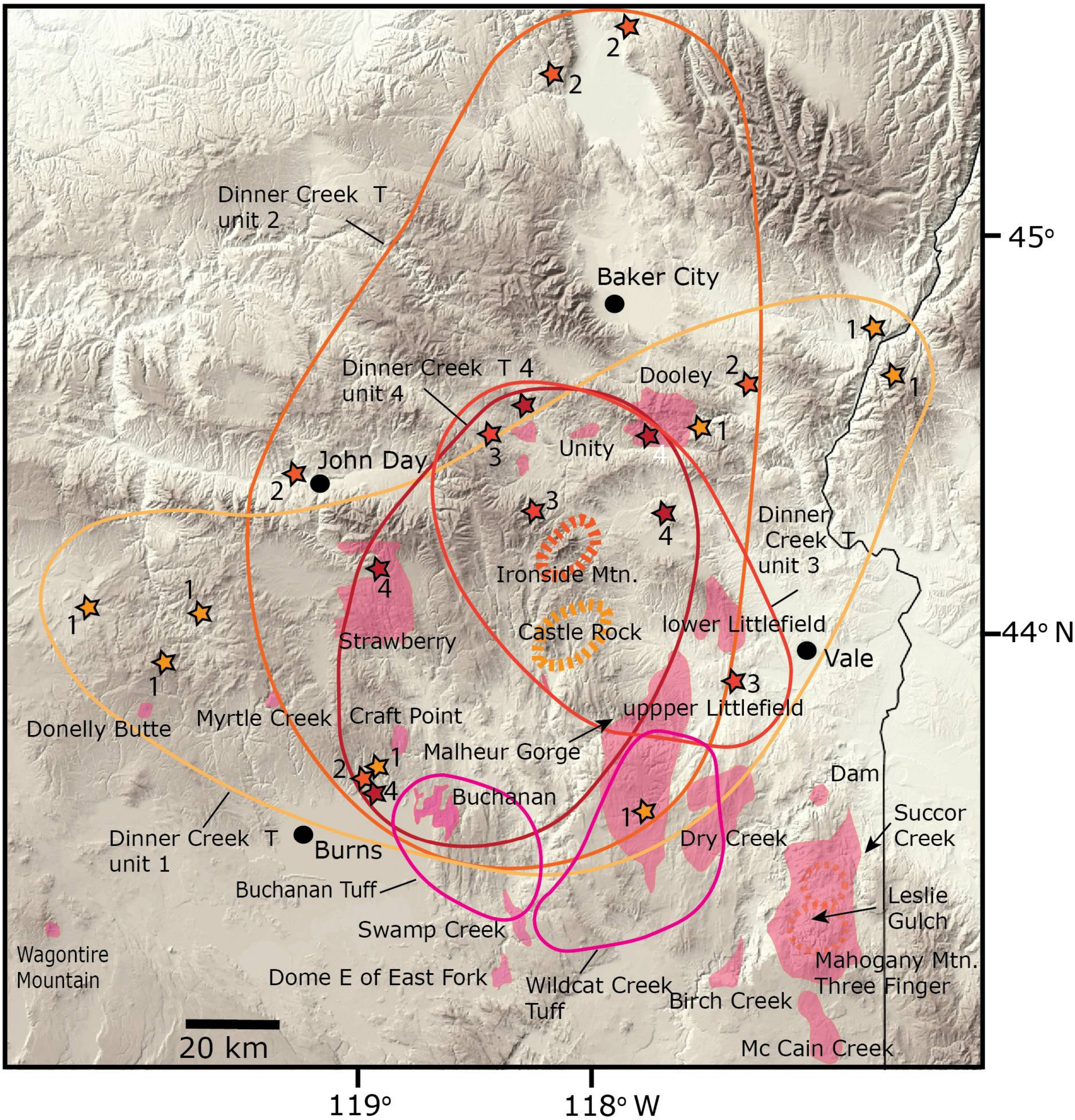

Figure 3. Location and extent of rhyolites investigated in this study; Solid lines represent the extent of ignimbrites with envelopes around the most distal outcrops of units of the Dinner Creek Tuff (stars), adapted from [51]. Dashed ovals indicate calderas (see text for details).

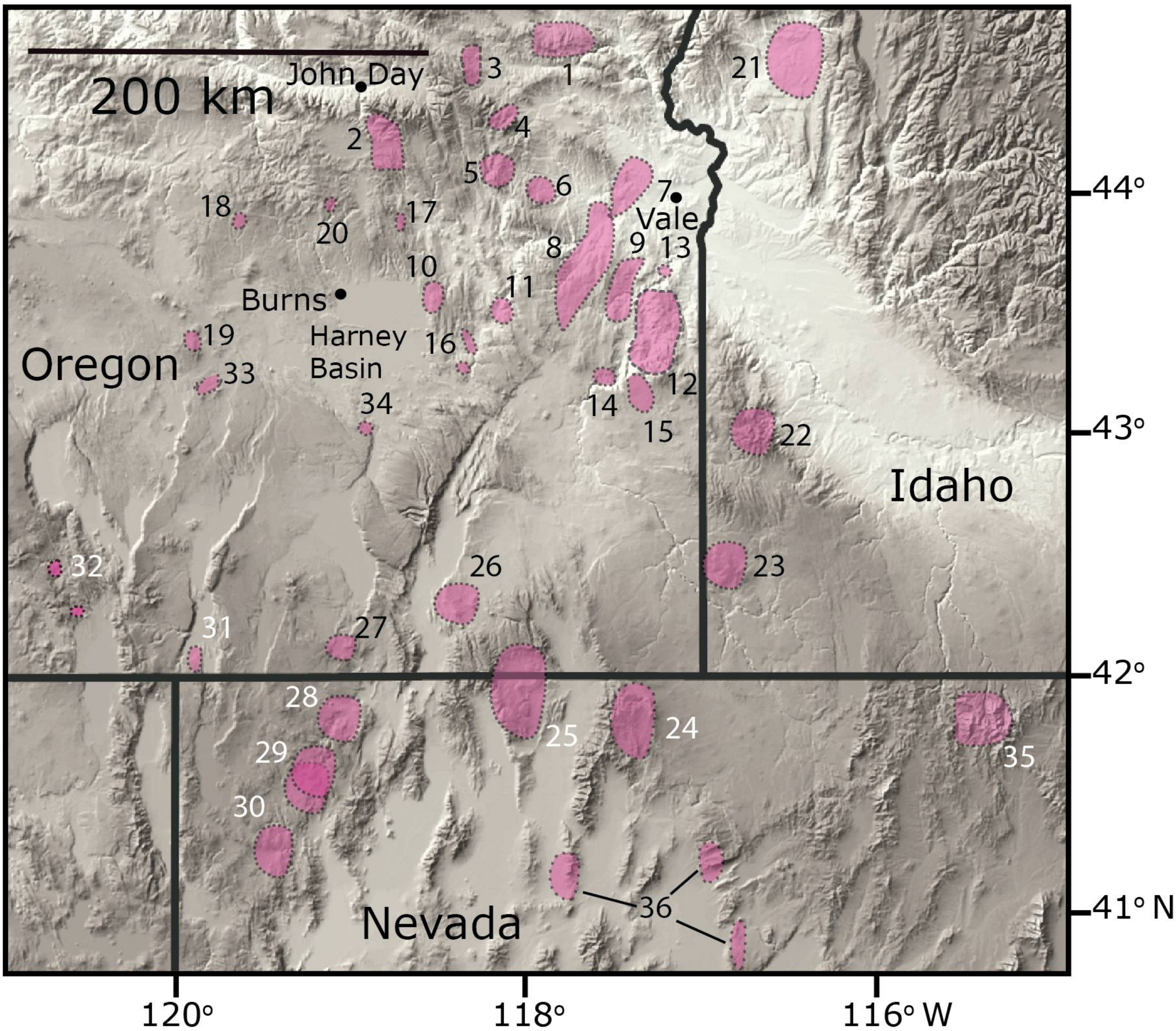

Figure 4. Map showing locations of all ~17–14.5 Ma rhyolite centers discussed in this paper. Centers labeled 1 through 20 are those that we studied; Centers 21 through 36 are based on the literature data mentioned in text. The centers are: 1: Dooley Mountain, 2: Strawberry, 3: Unity, 4: Ironside Mtn caldera (source of Unit 2 of Dinner Creek Tuff); 5: Castle Rock caldera (source of Unit 1 of Dinner Creek Tuff); 6: estimated source of Units 3 and 4 of Dinner Creek Tuff; 7: Lower Littlefield Rhyolite; 8: Upper Littlefield Rhyolite; 9: Dry Creek, 10: Buchanan; 11: estimated source of Wildcat Creek Tuff; 12: Mahogany Mountain—Three Fingers; 13: Dam; 14: Birch Creek; 15: McCain Creek; 16: Swamp Creek and Dome E of South Fork; 17: Craft Point; 18: Donnelly Butte; 19: Wagontire Mountain; 20: Myrtle Creek; 21: Weiser; 22: Silver City; 23: Juniper Mountain; 24: Santa Rosa Calico; 25: McDermitt; 26; N. McDermitt; 27: Hawks Valley; 28: High Rock; 29, 30, 31: Twenty Mile Creek; 32: Drumhill—Bald Butte; 33: Horsehead–Little Juniper Mountain; 34: Jackass Mountain; 35: Jarbidge; 36: 15–16 Ma rhyolites associated with ore deposits (see text for details).

A number of dikes crosscut older rhyolite units, one of which is a pyroclastic dike (Figure 5). The only previous date came from a dike near the summit of Dooley Mountain, yielding a K/Ar radiometric age of 14.7 ± 0.4 Ma [55]. Combining clear stratigraphic relationships and compositional characteristics, our work [54] yielded four compositional rhyolite packages, R1 through R4, from oldest to youngest, respectively (Figure 5). An R2 rhyolite yielded an age of $^{40}Ar/^{39}Ar$ age of 15.59 ± 0.04 Ma, and an R3 unit yielded an age of 15.54 ± 0.05 Ma. Two R4 units, the pyroclastic dike and a basal vitrophyric breccia, yielded ages of 15.491 ± 0.031 Ma and 15.44 ± 0.10 Ma, respectively. An additional R4 sample collected north of the main outcrop area yielded an age of 15.587 ± 0.059 Ma. We do not have an age of an R1 unit, as R1 lavas are extremely phenocryst-poor and the one sample that was processed yielded only sparse quartz phenocrysts. However, an R1 unit overlies unit 1 of the Dinner Creek Tuff with an age of 16.15 Ma in the southwest region of the field, providing a maximum age of R1. Based on our new Ar/Ar ages, the main portion of the rhyolite field at Dooley Mountain erupted very quickly over a period of ~200 ka. The main area of the Dooley Mountain rhyolite field is about 230 km^2. Evans [55] determined the rhyolite stratigraphy to be ~2400 m thick. However, we propose a more conservative estimate of 500–1000 m thick, yielding volume estimates of 115–230 km^3. Rhyolites range from low- to high-silica, and contrary to the findings of Evans [55], tuff units are clearly subordinate to dome and lava flows. Compositionally, Dooley Mountain rhyolites are in large part "calc-alkaline" rhyolite, characterized by low Y and Nb contents, although some variations—particularly in Zr and TiO_2—are notable. In select places, basalt lavas crop out below Dooley Mountain rhyolites. These have been mapped as Imnaha Basalt, but compositions of analyzed samples correlate better with the older or younger lavas of the Picture Gorge Basalt of the CRBG [54].

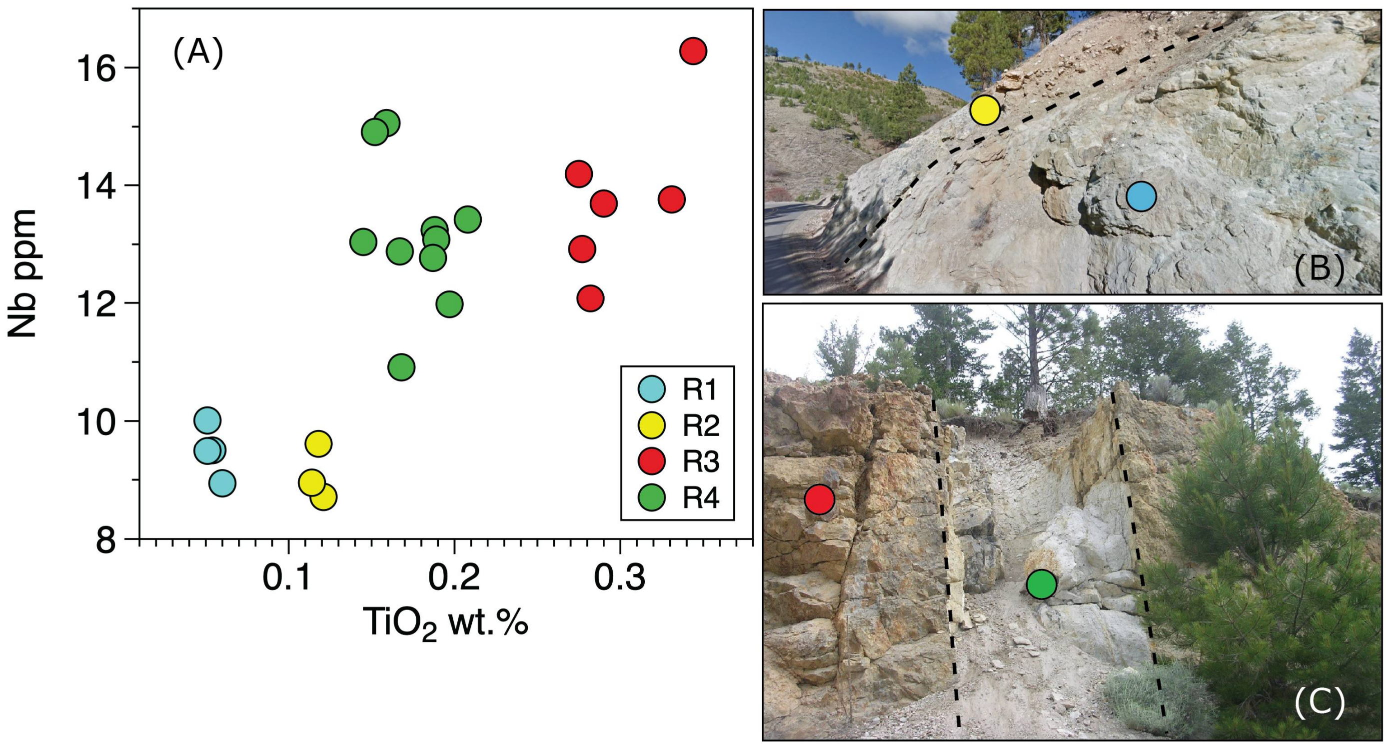

Figure 5. Field relationships and composition of Dooley Mountain rhyolites, the northernmost rhyolite center (after [54]). (**A**) Rhyolites are divided into 4 compositional groups, R1 through R4; (**B**) R2 rhyolite overlies R1 rhyolite; (**C**) Tuff dike with glassy matric and vertically oriented fiammes with a R4 composition cut rhyolite breccia of a R3 rhyolite.

3.1.2. Strawberry Rhyolite Field (2 in Figure 4)

The mid-Miocene Strawberry volcanic field (SVF) is located along the southern margin of the John Day Valley of NE Oregon, and it contains the northwesternmost rhyolites associated with CRBG lavas (Figures 3 and 4). The SVF is comprised of a diverse group of volcanic rocks ranging from basalt to rhyolite. Rhyolites were first mentioned as part of the Strawberry Volcanics in the 1960–70s (e.g., [56]), but neither their distribution, composition, nor ages were studied in detail. No subsequent work existed until our more recent work in the area. Building on our reconnaissance data obtained earlier [57], the main efforts to map rhyolites took place in the context of three USGS Edmap projects from 2019–2021 aided by Portland State University field study students. These maps covered the area of four 7.5 min quadrangles, including Jump off Joe Mountain, Big Canyon, Logan Valley West, and Magpie Table quadrangles [34,58,59].

Our study has revealed a major rhyolite field that is among the largest in Oregon (see Figures 16 and 17 of [60]). A minimum of 11 distinct effusive rhyolite units erupted over a 2-million-year period in addition to one mixed rhyolite–andesite pyroclastic deposit from ~16.2 to 14.4 Ma, and possibly as young as 14 Ma, as the stratigraphically highest rhyolite units are undated [61]. All but one of the nine new $^{40}Ar/^{39}Ar$ ages range from 15.4–14.4 Ma, with the majority falling into a narrow age range of about 500 ky (Table 1). Robyn [56] dated a sample from the larger rhyolitic section yielding a K/Ar age of 17.3 $\pm$ 0.36 Ma. However, this age is likely too old, as we specifically resampled the rhyolite location described by Robyn, and this sample yielded an age of 14.81 $\pm$ 0.04 Ma. Rhyolites overlie older rocks belonging to the accreted terranes of northeast Oregon (e.g., [61]). In the stratigraphically higher section, rhyolites are intercalated with basalt to andesite lavas of the SVF. The main andesitic lavas of the SVF overlie the rhyolites [34,57–59].

The mapped distribution of rhyolites covers an area of 190 km^2, but the estimated original distribution area is likely ~400 km^2, and the estimated volume is on the order of 100–200 km^3. Rhyolites range from low-silica to high-silica composition and from phenocryst-rich (>20% phenocrysts) to aphyric (Figure 6). All units display glassy to devitrified lithologies. Mineral assemblages are dominated by plagioclase; some units contain quartz, and mafic silicates often are amphibole, biotite, or both. Orthopyroxene occurs in some units in addition to or instead of biotite and amphibole [62]. Our data suggest the following age–volume–composition lithology relationships: Lower-silica, phenocryst-rich units containing complexly zoned plagioclase erupted early, while phenocryst-poorer and silica-rich units were more prevalent later. Units with slight A-type affinities erupted last.

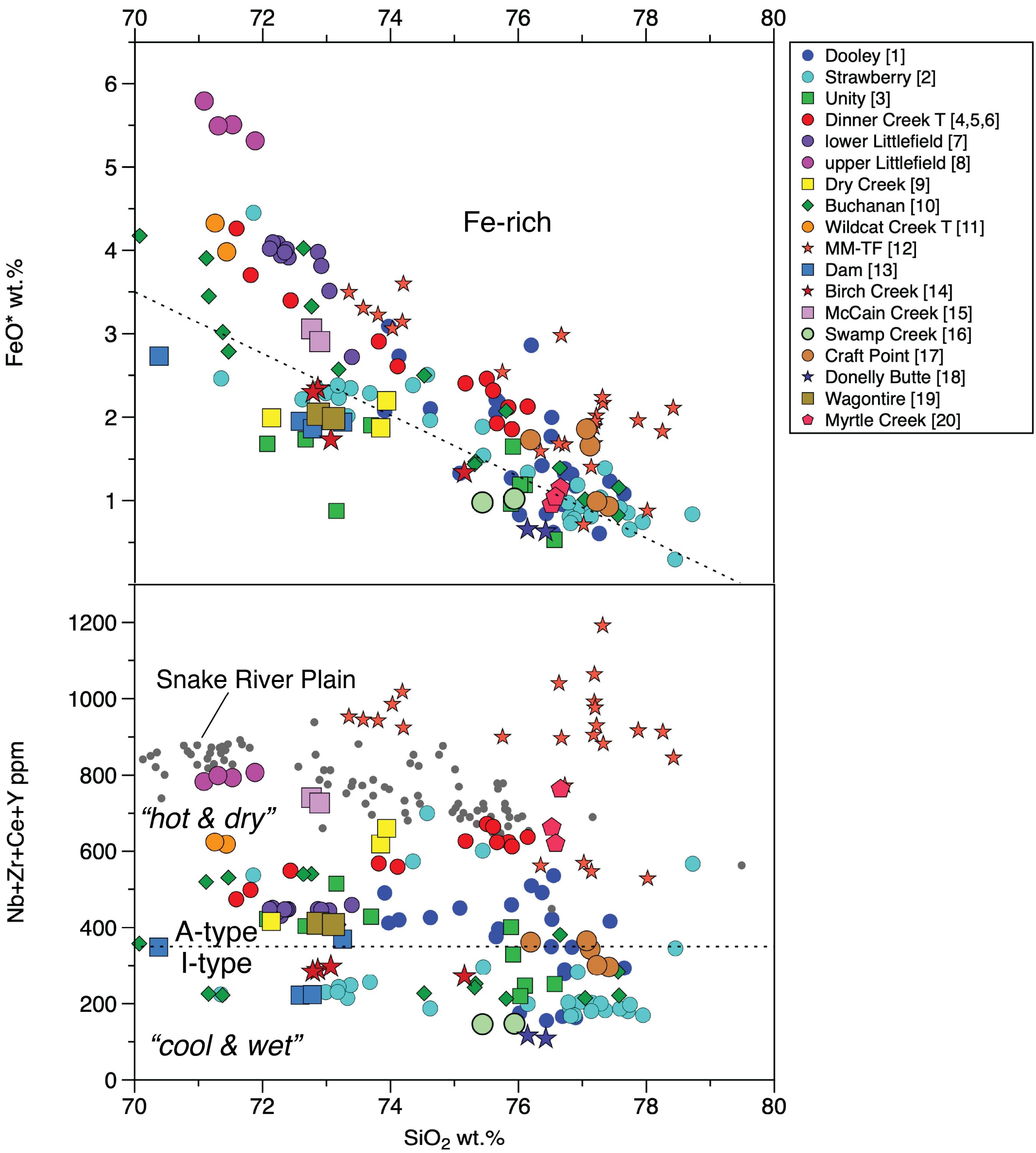

Figure 6. Composition of mid Miocene rhyolites of this study, FeO* is total Fe calculated as FeO; number in legend corresponds with location numbers in Figure 4. Rhyolites range from Fe-rich, A-type rhyolites to calcalkaline (Fe-poor, I-type) rhyolites. Line separating Fe-rich from Fe-poor varieties based on the line separating Iceland data from Cascades data taken from [63]. Line separating A-from I-type based on Whalen et al. [64]. Data for age-progressive Snake River Plain rhyolites from [4] are superimposed on lower panel. Calc-alkaline rhyolites mentioned in this paper do not have a direct counterpart in Idaho [42]. MM-TF: Mahogany Mountain–Three Fingers rhyolite field.

3.1.3. Unity Area Rhyolites (3 in Figure 4)

Between the rhyolite fields of Dooley Mountain and Strawberry, there are small rhyolite exposures north and west of the town of Unity, Oregon (Figures 3 and 4). These rhyolites were also virtually unknown and are not found on any regional-scale geological map of the area. Some of the rhyolites have been noted on a map of an MS thesis project [65] and others are based on our investigations. Most of the rhyolites in this area carry biotite or amphiboles, and they are compositionally similar to Dooley Mountain and Strawberry rhyolites. Together, they comprise not more than an a few km^2 of outcrop area. They overlie Oligocene phenocryst-rich dacites and underlie units of Dinner Creek Tuff, and they were emplaced to the west adjacent to mafic to intermediate lavas of SVF. Intriguingly, these small rhyolite exposures yielded our oldest CRBG related rhyolite ages. An Ar/Ar incremental heating age of one biotite–rhyolite tuff yielded an age of 16.53 ± 0.14 Ma. Two different rhyolite lavas yielded single-crystal $^{40}Ar/^{39}Ar$ ages of 16.695 ± 0.010 Ma and 17.02 ± 0.14 Ma. Compositionally, they are also more calc-alkaline in character, similarly to the two previous fields.

3.1.4. Buchanan Rhyolite Complex (10 in Figure 4) and Nearby Centers to the South (16 in Figure 4)

Previous work on the Buchanan rhyolite complex was limited to regional mapping [66,67] and brief mention of the possibility of multiple eruptive units [44]. As part of our work, Large [54] used stratigraphic relationships, geochemical analysis, and petrographic data to identify eight distinct rhyolite eruptive units (Figure 7). Of these, seven are effusive units consisting of mostly lava flows and possibly one dome. The last rhyolite unit is a local pyroclastic fallout unit composed of primarily lapilli- and ash-sized particles, with rare block-sized clasts. The size of these fragments varies over short distances within the complex, suggesting a local derivation. Lava flows have relatively low aspect ratios, and they include low- to high-silica rhyolites, ranging from aphyric to containing ~10% phenocrysts [54]. The slight differences observed in FeO*, TiO_2, Ba, Sr, Zr, Nb, and LREE are used to differentiate eruptive units. The rhyolites of the Buchanan complex are overlain by the commingled Fe-rich dacite–rhyolite tuff of Buchanan (15.171 ± 0.013 Ma), by a capping basalt that was dated at 13.79 ± 0.09 Ma [68], and by the widespread 9.7 Ma Devine Canyon Tuff [39] along the southeastern periphery of the complex. Newly obtained Ar/Ar ages indicate the basal rhyolite unit (R1 of [54]) erupted at 16.13 ± 0.11 Ma [69], then the middle unit (R4) at 15.803 ± 0.014 Ma, followed by the top rhyolite unit (R8) shortly after at 15.62 ± 0.31 Ma (Table 1 and Figure 7). Rare exposures of intercalated or underlying mafic lavas have been correlated with upper Steens Basalt [54]. The overall extent of rhyolite exposures, including areas between rhyolites that are covered by overlying units, is approximately 400 km^2. When excluding these unexposed areas to calculate a more equant distribution, the calculated areal estimate of rhyolites in the area is 150 km^2, which is still likely a minimum. Using estimated thicknesses of 100–300 m results in a calculated rhyolite volume between 15 km^3 and 45 km^3 for this complex.

Two calc-alkaline rhyolites, the Swamp Creek rhyolite and Dome E of South Fork, crop out about 20 km and 40 km to the southwest of the Buchanan complex, respectively. The Swamp Creek rhyolite was mapped by Camp et al. [16], and an older K/Ar age of 16.1 ± 0.3 Ma was reported by Fiebelkorn [13]. Our new age for the Swamp Creek rhyolite of 16.14 ± 0.12 Ma confirms the older age [69]. No prior work was conducted on the Dome E of South Fork, and our new work yielded an age of 16.81 ± 0.05 Ma, which is among the oldest reported for any CRBG-related rhyolite [34]. Similar to other small rhyolite occurrences further west, the Swamp Creek rhyolite and the Dome E of South Fork are comprised of a small outcrop area not larger than a few km^2, but this is unlikely their original extent given the coverage by younger regional ignimbrites and mafic lava flows.

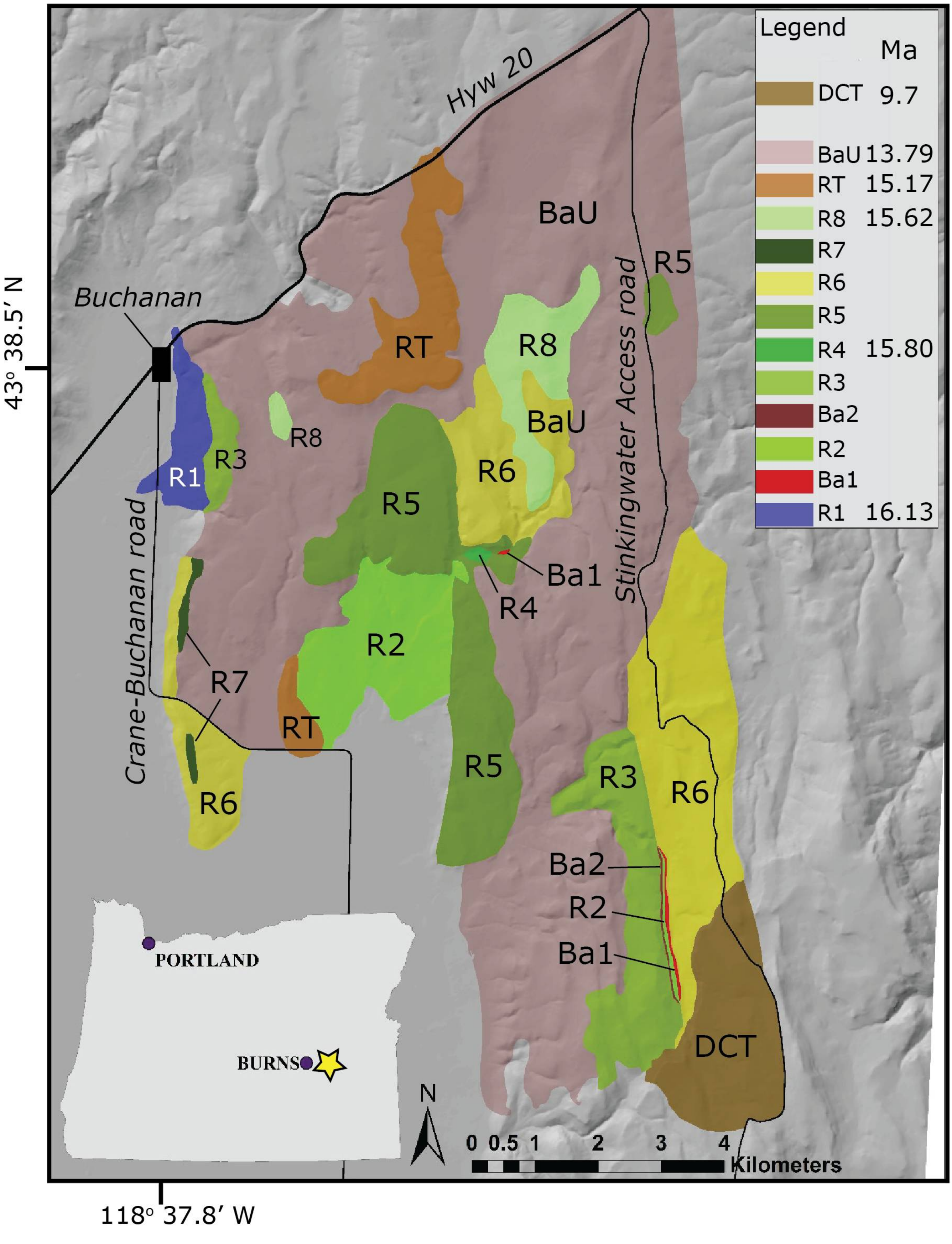

Figure 7. Map of Buchanan rhyolite complex with distribution of all rhyolite units [54] and new ages of this study, Hess [69], and Wright et al. [68] for age of basalt overlying rhyolites. R is rhyolite units, Ba is basaltic units, and DCT is regional Devine Canyon Tuff.

Table 1. $^{40}Ar/^{39}Ar$ age data of this study.

Dooley Mountain	Sample #	Location/Unit	Material	Age [FCT 28.2]	2 Sigma	Method	K/Ca	2 Sigma	N	Lab/Year	Reported by
Dooley	EJ-12-23A	R2 unit	Sanidine	15.59	0.04	weighted plateau	41.7			OSU	[69]
Dooley	DM 240	R3 unit	Plagioclase	15.539	0.047	single crystal	0.11	0.02	49	NMT	this study
Dooley	DM 265A	R4 unit	Plagioclase	15.44	0.10	single crystal	0.13	0.01	26	NMT	this study
Dooley	MS-11-22	R4 unit (tuff dike)	Plagioclase	15.491	0.031	single crystal	0.13	0.02	36	NMT	this study
Dooley	MS-17-14	R4 unit, north patch	Plagioclase	15.587	0.059	single crystal	0.12	0.02	28	NMT	this study
Unity	**Sample #**	**Location/unit**	**Material**	**Age [FCT 28.2]**	**2 sigma**	**Method**	**K/Ca**	**2 sigma**	**N**	**Lab**	**Reported by**
Unity	CR-U4b	below DIT2 tuff	Plagioclase	16.53	0.14	weighted plateau	0.15			OSU	[69]
Unity	CR-U3B		Sanidine	16.695	0.010	single crystal	47	51	5	NMT	this study
Unity	MS-12-14UR		Plagioclase	17.02	0.14	single crystal	0.08	0.05	12	NMT	this study
Strawberry	**Sample #**	**Location/unit**	**Material**	**Age [FCT 28.2]**	**2 sigma**	**Method**	**K/Ca**	**2 sigma**	**N**	**Lab**	**Reported by**
Strawberry	AS-SV-144		Plagioclase	15.34	0.52	weighted plateau	0.039			OSU	[70]
Strawberry	AS-SV-151		Groundmass	16.16	0.17	weighted plateau				OSU	[70]
Strawberry	AS-SV-151		Plagioclase	16.12	0.7	weighted plateau	0.04			OSU	[70]
Strawberry	AS-SV-173		Biotite	14.70	0.13	weighted plateau				OSU	[70]
Strawberry	AS-SV-179		Groundmass	15.30	0.1	weighted plateau				OSU	[70]
Strawberry	AS-SV-190		Groundmass	14.79	0.12	weighted plateau				OSU	[70]
Strawberry	MS-14-23		Obsidian	14.81	0.04	weighted plateau	8			NMT	[70]
Strawberry	JJ-17-8		Plagioclase	14.463	0.037	single crystal	0.05	0.04	17	NMT	this study
Strawberry	MS-17-05		Plagioclase	15.112	0.030	single crystal	0.11	0.05	25	NMT	this study
Upper/Lower Littlefield Rhyolite	**Sample #**	**Location/unit**	**Material**	**Age [FCT 28.2]**	**2 sigma**	**Method**	**K/Ca**		**N**	**Lab**	**Reported by**
upper Littlefield Rhyolite	multiple samples			16.05							[71]
lower Littlefield Rhyolite	multiple samples			16.15							[71]
Buchanan	**Sample #**	**Location/unit**	**Material**	**Age [FCT 28.2]**	**2 sigma**	**Method**	**K/Ca**		**N**	**Lab**	**Reported by**
Buchanan	EJ-12-03	R1 unit	Sanidine	16.13	0.11	weighted plateau	41.7			OSU	[69]
Buchanan	B156	R4 unit	Sanidine	15.803	0.014	single crystal	20.6	2.2	25	NMT	this study
Buchanan	B109	R8 unit	Plagioclase	15.62	0.31	single crystal	0.09	0.05	15	NMT	this study
tuff of Buchanan	MS-13-07	tops lava flow complex	Anorthoclase	15.171	0.013	single crystal	3.9	1.5	25	NMT	this study
Mahogany-Three Fingers Succor Creek area	**Sample #**	**Location/unit**	**Material**	**Age [FCT 28.2]**	**2 sigma**	**Method**	**K/Ca**		**N**	**Lab**	**Reported by**
Mahogany-Three Fingers	EJ-12-12	Devils Gate	Anorthoclase	15.94	0.16	weighted plateau	6.6			OSU	[69]
Mahogany-Three Fingers	TF88A	Three Fingers (TF)	Sanidine	15.74	0.08	weighted plateau	41.2			OSU	[72]
Mahogany-Three Fingers	EJ-12-14	McIntyre Ridge	Sanidine	15.78	0.03	single crystal	20	12.9	11	NMT	this study

Table 1. *Cont.*

Mahogany-Three Fingers Succor Creek area	Sample #	Location/Unit	Material	Age [FCT 28.2]	2 Sigma	Method	K/Ca	2 Sigma	N	Lab/Year	Reported by
Mahogany-Three Fingers	MS-11-15SCT	Succor Creek Tuff	Anorthoclase	15.74	0.09	weighted plateau	6.2			OSU	[72]
Mahogany-Three Fingers	CB-18-02	base of LGT at Succor Creek	feldspar	15.98	0.05	single crystal				OSU	[73]
Mahogany-Three Fingers	CB-19-65	Devils Gate	feldspar	16.02	0.02	single crystal				OSU	[73]
Mahogany-Three Fingers	CB-19-44		feldspar	15.95	0.03	single crystal				OSU	[73]
Mahogany-Three Fingers	MS-10-06	"outflow" LTG	Sanidine	15.87	0.03	single crystal	7.3	2.5	10	NMT	this study
Leslie Gulch area and nearby	**Sample #**	**Location/unit**	**Material**	**Age [FCT 28.2]**	**2 sigma**	**Method**	**K/Ca**		**N**	**Lab**	**Reported by**
Mahogany-Three Fingers	RJ-18-03	Mahogany Mountain	feldspar	15.71	0.05	single crystal				OSU	[74]
Mahogany-Three Fingers	RJ-18-05	Mahogany Mountain	feldspar	15.83	0.04	single crystal				OSU	[74]
Mahogany-Three Fingers	RJ-18-11	Mahogany Mountain	feldspar	15.81	0.06	single crystal				OSU	[74]
Mahogany-Three Fingers	RJ-18-50	Mahogany Mountain	feldspar	15.82	0.05	single crystal				OSU	[74]
Mahogany-Three Fingers	MS-12-39b	Tuff of Leslie Gulch	Sanidine	15.948	0.037	single crystal	9.5	3	6	NMT	this study
Mahogany-Three Fingers	MS-13-27	tuff below TF	Sanidine	15.928	0.007	single crystal	228	148	14	NMT	this study
Mahogany-Three Fingers	MS-17-15	Pre-LTG lava	Sanidine	16.042	0.016	single crystal	9.50	2.00	29	NMT	this study
Dinner Creek Tuff (DIT)	**Sample #**	**Location/unit**	**Material**	**Age [FCT 28.2]**	**2 sigma**	**Method**	**K/Ca**		**N**	**Lab**	**Reported by**
Unit 1	MS-12-29.1	at Brogan	An10 plag	16.16	0.02	single crystal	0.73		9	NMT	[19]
Unit 1	MS-DIT1	type locality	An10 plag	16.120	0.026	single crystal	0.74	0.09	36	NMT	this study
Unit 2	MS-15-12.3	capping Spying Glass CRBG flow	An20 plag	15.653	0.038	single crystal	0.2	0.1	35	NMT	this study
Unit 3	MS-12-38	at Bully Creek	Anorthoclase	15.458	0.021	single crystal	2.65			NMT	[19]
Unit 4	MS-11-20		Anorthoclase	15.173	0.010	single crystal	14.7	74.2	11	NMT	this study
Other ages with lower precision are found in [19], but all are displayed in Figure 8.											
Various units	**Sample #**	**Location/unit**	**Material**	**Age [FCT 28.2]**	**2 sigma**	**Method**	**K/Ca**		**N**	**Lab**	**Reported by**
Birch Creek	V19-068		Plagioclase	15.52	0.05	single crystal			29/30	OSU	[34]
Birch Creek	V19-079		Plagioclase	14.94	0.2	single crystal			29/30	OSU	[34]
McCain Creek	RJ-18-57		feldspar	14.41	0.04	single crystal				OSU	[74]
Lake Owyhee Dam	MS-17-DAM		Plagioclase	14.74	0.02	single crystal			30/30	OSU	[34]
Dry Creek	VS19-116		Plagioclase	14.78	0.03	single crystal			24/30	OSU	[34]
Beulah Reservoir	EJ-12-07	pre-DIT caldera rhyolite	Groundmass	16.29	0.21	weighted plateau				OSU	[69]
Swamp Creek	EJ-12-06A		Obsidian	16.14	0.12	weighted plateau/total fusion				OSU	[69]
Dome E of South Fork	VS19-080		Groundmass	16.81	0.05	weighted plateau			-	OSU	[34]
Wildcat Creek Tuff	MS-14-05		Anorthoclase	15.489	0.022	single crystal	2.3	0.8	13	NMT	this study
Donnelly Butte	EJ-12-02		Groundmass	15.59	0.06	weighted plateau				NMT	[34]
Wagontire Mountain	VS20-125A		Plagioclase	14.79	0.05	single crystal			25/30	OSU	[34]

3.1.5. Dinner Creek Tuff (4, 5, 6 in Figure 4)

The Dinner Creek Tuff was first described in the 1960s and 70s and was originally restricted to the Castle Rock and Malheur River Gorge area, with a maximum areal distribution of about 2000 km^2 [75,76]). Field work in the following decades expanded the area of the tuff; grouped it into the LOVF along with several other regionally extensive rhyolitic tuffs, lava flows, and domes; and postulated a source caldera near Castle Rock despite a lack of any field evidence [43,77,78]. The only published field work that existed to support this interpretation was based on the MS thesis work by Woods [76], who interpreted the prominent physiographic feature of Castle Rock and other nearby outcrops of Dinner Creek Tuff as dikes and sources for the tuff.

Our new work on distribution, lithologic variations, geochemical compositions, and eruption ages indicates that the extensive Dinner Creek Tuff, along with correlated mapped and unmapped ignimbrites, includes a minimum of four discrete cooling units that were emplaced over an area of about 32,000 km^2 (Figures 3 and 8) [19,79]. Three of the four units are low- to high-silica rhyolites. The youngest unit posses a dacite bulk composition, which is due to commingling of rhyolites with andesitic mafic components [19]. Widespread fallout deposits in northeast Oregon and the neighboring states of Nevada, Idaho, and Washington have now been compositionally correlated with the redefined Dinner Creek Tuff [19]. Compositional coherence among rhyolites of the ignimbrite sheets and fallout deposits indicates a common source area [19] (Figure 6). Our subsequent work identified the Castle Rock caldera formed during the eruption of the 16.16 Ma Dinner Creek Tuff Unit 1 [80]. The northwestern boundary of the caldera is roughly defined by the juxtaposition of over 300 m of densely welded rheomorphic intra-caldera tuff and tuffaceous megabreccia deposits against Mesozoic Weathersby Formation shale and pre-Miocene Ring Butte trachybasalt lavas. Following caldera collapse, fluvial and lacustrine volcaniclastic sediments were deposited on the caldera floor, and outflow tuffs of the Dinner Creek Tuff Units 2 and 4 were deposited in the caldera. Aphyric basaltic andesite and icelandite (Fe-rich andesite), which stratigraphically correlate to upper Grande Ronde Basalt lavas, intrude the caldera floor deposits, and lavas are interbedded with sediments and Dinner Creek Tuff Unit 4. The Ironside Mountain caldera formed during the eruption of 15.6 Ma Dinner Creek Tuff Unit 2, ~15 km north of the Castle Rock caldera [81]. The caldera is an 11 km by 6 km depression wherein over 900 m of intracaldera, rheomorphic, and partially welded tuff are bound by Weathersby Formation shale and Tureman Ranch granodiorite. Post-caldera collapse, basaltic andesite and icelandite dikes and sills, also stratigraphically correlative to upper Grande Ronde Basalt lavas, intruded into the tuff, mostly along the margins of the caldera, altering much of the tuff. Identification of source areas for the 16.46 Ma Unit 3 and the 15.2 Ma Unit 4 of the Dinner Creek Tuff is outstanding, but it appears to be southeast of the Castle Rock caldera (cf. Figure 3) [81]. Minimum areas for individual units are as follows: ~22,600 km^2 (Unit 1), ~17,900 km^2 (Unit 2), ~10,400 km^2 (Unit 3), and ~9300 km^2 (Unit 4). Using conservative thicknesses, determined tuff volumes are ~170 km^3 (Unit 1), ~112 km^3 (Unit 2), ~65 km^3 (Unit 3), and ~58 km^3 (Unit 4), totaling ~405 km^3 (dense rock equivalent). Minimum calculated caldera volumes for Units 1 and 2 are ~99 km^3 (Unit 1) and ~31 km^3 (Unit 2), increasing the erupted volumes to ~269 km^3 for Unit 1 and to ~143 km^3 for Unit 2 [51].

A pre-caldera rhyolite lava older than the Dinner Creek Tuff crops out just south of Castle Rock, where we obtained an age of 16.29 $\pm$ 0.21 Ma (Table 2).

Cognate mafic components (glass shards, pumice shards, and mafic globules) that range in composition from dacite (~68 wt % SiO_2) to Fe-rich basaltic andesite (~56 wt % SiO_2) in composition are found in two of the cooling units (Figure 9). Major and trace element compositions of the more mafic components match the composition of nearby Grande Ronde Basalt flows and dikes. Compositional similarities between cognate mafic components and Grande Ronde Basalt flows are direct evidence for coeval mafic and silicic magmatism, linking rhyolites of the Dinner Creek Tuff and Grande Ronde Basalt eruptions. Furthermore, finding Grande Ronde Basalt magmas as co-eruptive component in Dinner

Creek Tuff suggests that Grande Ronde Basalt magmas were stored beneath Dinner Creek Tuff rhyolites, thereby providing the first direct evidence for the location of a storage site of Columbia River Basalt magmas. Rhyolites of the Dinner Creek Tuff are Fe-rich and have A-type affinity (Figure 6).

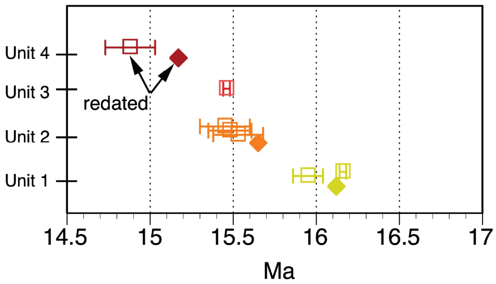

Figure 8. Ages of Dinner Creek Tuff units after [19] and 2 sigma error bars. Solid diamonds for new ages reported here. Two sigma errors of new ages are within symbol size.

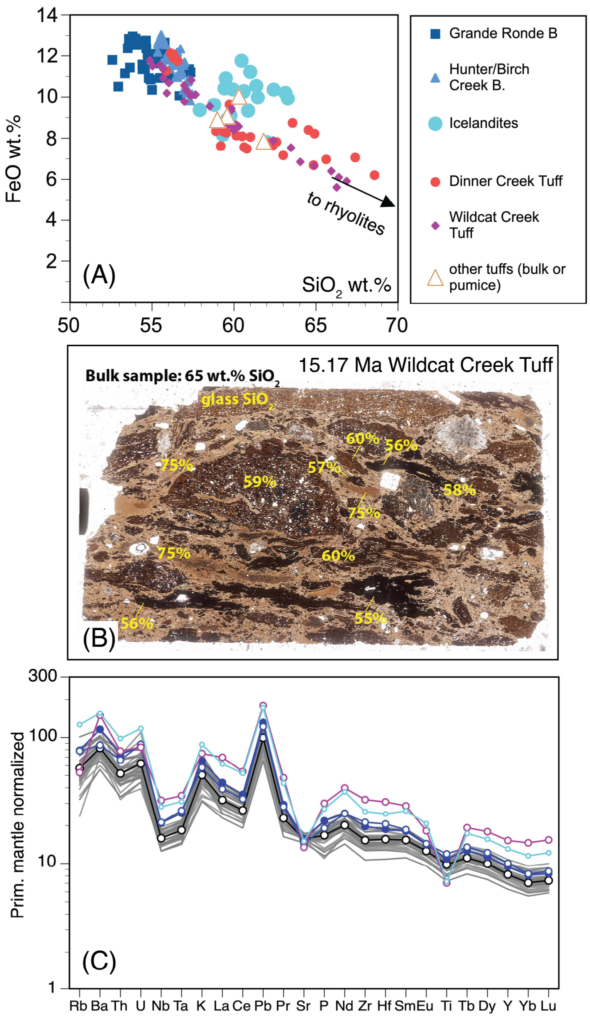

Figure 9. (**A**) Geochemical correlation of local basaltic units (Hunter Creek and Birch Creek Basalt) [71] with Grand Ronde Basalt [11] and relationships to locally erupted icelanditic lavas and tuff components; (**B**) thin section image (plane polarized light) showing commingled, icelandite–rhyolite, components in the Wildcat Creek Tuff [81]; (**C**) mantle normalized incompatible trace element diagram comparing Grande Ronde Basalt lavas (gray lines; black for average composition) [11] with averages of local Grande Ronde units (solid blue dots for Birch Creek lavas; open blue dot for Hunter Creek Basalt), local icelandite lava (light blue), and icelandititic component of Wildcat Creek Tuff (magenta line).

Table 2. Summary of duration of activity of rhyolite centers. Dark areas indicate activity of this center in this time slot. Numbers in the brackets refer to the numbers of rhyolite centers of Figure 4.

Northern Sector (43°–45° N)	**Activity Phase, Ma**			
This Study	**17.5–16.4**	**16.3–15.9**	**15.8–15.4**	**15.3–14.5**
Dooley Mountain (1)			■	■
Strawberry (2)		■	■	■
Unity (3)	■			
Ironside Mtn (4)			■	
Castle Rock (5)		■		
Source for Units 3 and 4 of Dinner Creek Tuff (6)			■	■
Lower Littlefield (7)		■		
Upper Littlefield (8)		■		
Dry Creek (9)				■
Buchanan and Buchanan tuff (10)		■	■	■
Wildcat Creek tuff source (11)			■	
Mahogany Mountain—Three Fingers (12)		■	■	
Owyhee Dam "Dam" (13)				■
Birch Creek (14)			■	■
McCain Creek (15)				■
Swamp Creek and Dome E of South Fork (16)	■	■		
Craft Point (17)		■		■
Donnelly Butte (18)			■	
Wagontire Mountain (19)				■
Myrtle Creek (20)		**???**	**???**	
Literature				
Weiser (21)	■			
Silver City (22)	■			■
Horsehead and Little Juniper Mountain (33)			■	
Jackass Butte (34)			■	
Southern Sector (43°–41° N) Literature	**Activity Phase, Ma**			
	17.5–16.4	**16.3–15.9**	**15.8–15.4**	**15.3–14.5**
Juniper Mountain (23)				■
Santa Rocsa—Calico (24)	■	■	■	
McDermitt (proper) (25)	■	■		
Whitehorse (McDermitt, N) (26)	■	■	■	
Hawks Valley (27)	■			
Virgin Valley (28)	■			
High Rock or Badger Mountain/Hanging Rock (29)	■	■	■	
Cottonwood Creek (30)		■	■	■
Twelve Mile Creek (31)				■
Drumhill and Bald Butte (32)	■			

3.1.6. Littlefield Rhyolite (7 and 8 in Figure 4) and Wildcat Creek Tuff (11 in Figure 4)

The Littlefield Rhyolite, named by Kittleman et al. [75], is an extensive unit consisting of rhyolite lava flows north and south of the eastern Malheur Gorge, eastern Oregon (e.g., [77]) (Figures 3 and 10). Although Lees [82] found geochemical evidence for the existence of an older and younger magma type of the Littlefield Rhyolite, subsequent publications did not adopt the division into lower (older) and upper (younger) rhyolite units [8,16,18].

Although indistinguishable in the field, the Littlefield Rhyolite indeed consists of two distinct, voluminous, Fe-rich, Snake-River-type (cf. [83,84]), high temperature rhyolite lava packages that are currently referred to as the Lower and Upper Littlefield Rhyolite. The Lower and Upper Littlefield Rhyolites erupted in short succession (over less than 100 ka), with areal distributions of ~800 and ~1000 km^2 and minimum volumes of 100 and 150 km^3, respectively. The two rhyolites are clearly distinguished by composition (e.g., by Zr, Ba, Nb, TiO_2 and FeO) but also by mineral composition and $^{40}Ar/^{39}Ar$ ages (16.11 Ma for the lower and 16.02 Ma for the upper Littlefield Rhyolites, respectively) (Figure 6) [71].

Figure 10. (**A**) Type section of upper and lower Littlefield Rhyolite (LFR) lava flows along Highway 20 in Malheur Gorge, west of Vale (Figure 3), which reveals an intricate basalt–rhyolite stratigraphy (after [71]). Entire section is 250 m thick. HCB = lavas and tuffs of Hunter Creek Basalt (aka late, or upper Grande Ronde unit). Dinner Creek Tuff Unit 1 and Birch Creek Basalt (aka late, or upper Grande Ronde unit) underlie the lower LFR to the left of outcrop of picture. (**B**) Area around type section of (**A**); most of the outcrops in the figure are LFR, and the location of (**A**) is highlighted by white dashed rectangle.

On the other hand, rhyolites known either as "rhyolite of Cottonwood Mountain" or "rhyolite of Bully Creek Canyon", which are exposed around Cottonwood Mountain, northwest of Vale (cf. [8]), have identical compositions to samples of the Lower Littlefield Rhyolite. Single-crystal $^{40}Ar/^{39}Ar$ ages of two samples (16.12 ± 0.07 Ma and 16.20 ± 0.08 Ma) are statistically indistinguishable. This demonstrates that the rhyolites of Cottonwood Mountain and Bully Creek Canyon are, in fact, the Lower Littlefield Rhyolite. Thus, a more accurate recalculation of minimal extent of the Lower Littlefield Rhyolite is a distance of 40 km from vents observed within the Malheur River Gorge in the south to Cottonwood Mountain in the north.

A number of other rock units are sandwiched between the Lower and Upper Littlefield Rhyolite, where they crop out in sequence near the historic town of Namorf in the Malheur Gorge (Figure 10). These units include several basaltic lava flows and a one-meter-thick agglutinated spatter deposit of local Grande Ronde Basalt. The spatter deposit thickens to tens of meters over a distance of 800 m, where the deposit is strongly welded. We now recognize this as a venting site of Grande Ronde Basalt. Ages of Littlefield Rhyolite flow units bound the timing of eruption of local Grande Ronde Basalt to a span of ~100 ka between 16.05–16.12 Ma, and they provide a narrow age constraint on the controversial lower age of Grande Ronde Basalt volcanism.

The Upper Littlefield Rhyolite is overlain in the southwest of its distribution area by another Fe-rich dacite–rhyolite-commingled ignimbrite, the Wildcat Creek Tuff. The tuff was undated, and only a stratigraphic age existed. We obtained an age of 15.489 ± 0.022 Ma via Ar/Ar single-crystal analysis on anorthoclase. The bulk composition of the tuff varies from 62 to 71 wt.% SiO_2, but the bulk composition represents commingling of 74 wt.% SiO_2 rhyolite with Fe-rich ~60 wt.% dacite magmas, leading to a spectacular-looking dark tuff (Figure 9). Dinner Creek Tuff Unit 4 (best age 15.24 Ma) and the tuff of Buchanan (15.12 Ma) (see above) are similarly commingled, with dacitic to low-Si rhyolite bulk compositions.

3.1.7. Mahogany Mountain—Three Fingers (12 in Figure 4) and Nearby Rhyolite Fields (9, 13, 14, 15 in Figure 4)

The ~900 km^2 Mahogany Mountain—Three Fingers rhyolite field (MM–TFrf) is one of largest mid-Miocene rhyolite centers associated with Columbia River flood basalt volcanism (Figures 3 and 4). Early studies advocated for a two-caldera model consisting of the Mahogany Mountain caldera and the younger Three Fingers caldera producing the tuff of Leslie Gulch (TLG) and the tuff of Spring Creek, respectively, along with pre- and post-caldera effusive rhyolites [85,86]. Benson and Mahood [87] suggested only one larger caldera with pre- to post-caldera rhyolites after finding that the tuff of Spring Creek in Leslie Gulch proper is part of the TLG. Combining data from our recent studies [73,74] and results by Marcy [72], we can further address the stratigraphic and geochemical eruptive history of this rhyolite field.

The only rhyolite underlying the TLG is found in the Leslie Gulch locality (Figure 3) [7], yielding an age of 16.042 ± 0.016 Ma. All other, abundant and compositionally variable rhyolites of the MM–TFrf (Figure 6) post-date the tuff of Leslie Gulch, including the prominent rhyolites of Mahogany Mountain (15.82 ± 0.05–15.71 ± 0.05 Ma; Table 1) in the south and the rhyolite of McIntyre Ridge along the NW margin of the MM–TFrf (cf. [60]). Along Succor Creek (Figure 3), we correlate mostly nonwelded tuffs, that underlie pronounced rhyolite cliffs of McIntyre Ridge (15.86 ± 0.03 Ma) and of Devils Gate (e.g., 15.95 ± 0.03 Ma), with the TLG; tuffs consist of fine-grained ignimbrites, surges, and fallout deposit [73]. Stratigraphic data reveal that the TLG is a complex, multi-phase deposit with periodic pauses in eruptive activity. Ignimbrites distinct from the TLG range in age from 15.928 ± 0.007 Ma to 15.74 ± 0.09 Ma, and these tuffs indicate pyroclastic activity elsewhere in the MM-TTrf from the rhyolitic Honeycomb Hills [18] immediately north of the original Mahogany Mountain caldera to Succor Creek in the northeast.

The MM-TFrf represents a prolific rhyolite center that was active for 300 Ka, starting effusively at 16.04 Ma but quickly continuing with a major phreatomagmatic phase to deposit the composite TLG. This activity was followed by widespread post-caldera effusive rhyolites that were punctuated by other pyroclastic events (with or without caldera formation), all of which ended at ~15.7 Ma. The estimated volume for this main phase of the MM-TFrf is 300–500 km^3. All rhyolites of the MM-TFrf are Fe-rich, A-type rhyolites with A-type affinities becoming less pronounced with younger age (Figure 6).

Rhyolite eruptions recommenced to the southeast of the MM-TFrf with the 15.52 ± 0.02 Ma to 14.94 ± 0.2 Ma calc-alkaline Birch Creek rhyolite (14 in Figure 4) [34], to the south of the field with the 14.42 ± 0.02 Ma Fe-rich McCain Creek rhyolite (15 in Figure 4) [74], and in the northern portion of the field with the calc-alkaline Owyhee Dam rhyolite (aka Dam rhyolite) (13 in Figure 4) at 14.74 ± 0.02 Ma [34]. Our ages are largely consistent with recent Ar/Ar ages from [87], with our younger age of Birch Creek being the only exception.

Another rhyolite yielding an age of later-stage rhyolites that we associated with Columbia River Basalt magmatism is the Fe-rich rhyolite of Dry Creek [9] (14.78 ± 0.03 Ma, [34]), located between exposures of the lower Littlefield Rhyolite and the MM-TFrf (Figure 3).

3.1.8. Rhyolites along the Western Margin (17, 18, 19, 20 in Figure 4)

There are several mid-Miocene rhyolite centers that lie along the western periphery of CRBG-associated rhyolites. Each of these rhyolites is comprised of a small outcrop area not larger than a few km^2. However, this is unlikely their original extent as younger regional ignimbrites, mafic lava flows, and younger effusive rhyolites are found nearby and likely obscured these rhyolites. West, at 119.3° W, two dome complexes expose mid-Miocene rhyolites (Figures 3 and 4); 40 km north of the town of Riley, a small exposure of Donnelly

Butte (18 in Figure 4) with an Ar/Ar plateau age of 15.59 ± 0.06 Ma is surrounded by younger rocks. Wagontire Mountain (19 in Figure 4), located about 30 km south-southwest of Riley, is primarily comprised of several younger rhyolite units. Wagontire Mountain also contains an older, mid-Miocene portion that we could only sample along the western margin due to access issues. A glassy crystal-rich sample from Wagontire Mountain yielded an Ar/Ar age of 14.79 ± 0.05 Ma. Two rhyolites east and west of highway 395 and north of Burns currently do not have radiometric ages, but stratigraphic relationships indicate mid-Miocene ages (Figures 3 and 4). The previously unmapped calc-alkaline rhyolite of Craft Point (17 in Figure 4) crops out 30 km northwest of Burns, and it underlies Unit 1 of the Dinner Creek Tuff, assigning it a stratigraphic age of ≥ 16.2 Ma. Outcropping 30 km north of Burns, the Fe-rich rhyolite of Myrtle Creek (20 in Figure 4) clearly lies below the 9.7 Ma Devine Canyon Tuff but also likely below Unit 4 and Unit 1 of the Dinner Creek Tuff. Therefore, the stratigraphy suggests a 15–16 Ma age as well for the rhyolite of Myrtle Creek. The rhyolite of Craft point is a quartz-phenocryst bearing high-silica rhyolite straddling the calc-alkaline/A-type divide while the rhyolite of Myrtle Creek has a strong A-type trace element signature (Figure 6).

3.2. Ages of Other Mid-Miocene Silicic Centers

Here, we summarize the ages of other rhyolites emplaced in southeastern Oregon, northern Nevada, and western Idaho that fall into the ~17–~15 Ma age range. Some of these rhyolites have long been associated with CRBG magmatism, while ages of others became available only recently. All Ar/Ar ages were calculated with a Fish Canyon Tuff age of 28.201 Ma [88].

3.2.1. McDermitt Volcanic Field (25, 26 in Figure 4)

McDermitt Caldera has historically been viewed as the starting point of the Snake River Plain–Yellowstone age-progressive rhyolites, long interpreted to represent the Yellowstone Hotpot track [35]. Recent compiled mapping and age dating by Henry et al. [26] determined that rhyolite eruptive activity at McDermitt (proper) began with 16.6–16.7 Ma with pre-caldera lavas, followed by the main caldera forming ignimbrite eruption at ~16.35 Ma. Eruption of effusive post-caldera rhyolite and Fe-rich intermediate lavas followed shortly after emplacement of caldera-forming ignimbrite. Most of the rhyolites at McDermitt are peralkaline A-type rhyolites, but biotite-bearing calc-alkaline rhyolites also occur relatively early in the eruption sequence [26]. A study by Benson and Mahood [22] focusing on the greater McDermitt volcanic field also includes the Whitehorse Caldera of [78] and what they designate as the northern McDermitt volcanic field [26] in addition to the rhyolites of McDermitt Caldera that they label southern McDermitt volcanic field [31] and for which they obtained matching age data. Their additional ages of rhyolites from the northern McDermitt volcanic field reiterate that effusive eruptions began at 16.6 Ma, followed by alternating ignimbrite and effusive eruptions, culminating with the caldera-forming ignimbrite associated with the Whitehorse caldera at ~15.6 Ma.

Tuffs from the southern and northern volcanic field interfinger, and this has led to different views on the number of eruptive units, their origins, and what to call them (cf. [22,26]).

3.2.2. High Rock Caldera Complex (28–30 in Figure 4)

Fifty kilometers to the west of McDermitt Caldera lies a mid-Miocene caldera complex—the High Rock caldera complex, which has been known and studied for decades ([17] and references therein). The complex consists of three to four south-southwest-aligned calderas, each with associated pre- and post-caldera lava. The oldest pre-caldera rhyolite is 16.69 ± 0.15 Ma, preceding the eruption of the tuff of Idaho Canyon at ~16.49 [17] or at 16.56 Ma [26]; these eruptions came from Virgin Valley Caldera [17], the northeastern-most caldera of the complex [17]. The other ignimbrites with caldera formation erupted at ~16.45, ~16.1, and ~15.8 Ma. The last post-caldera effusive rhyolites erupted at ~15.8 Ma from Cottonwood Creek Caldera [80], the southwesternmost caldera [17]. Peak activity within the High Rock Caldera complex appears to be between 16.3 Ma and 15.9 Ma, and there is some disagreement on the total number of distinct calderas and ignimbrites [17,26].

3.2.3. Hawks Valley–Lone Mountain Volcanic Field (27 in Figure 4)

Just north of the High Rock caldera complex on the other side of the Oregon/Nevada state border is the Hawks Valley–Lone Mountain volcanic field [27], composed of a mostly effusive rhyolite–trachyte suite. Rhyolites here have yielded ages of 16.6–16.4 Ma [46].

3.2.4. Santa Rosa–Calico Volcanic Field (24 in Figure 4)

Twenty to thirty kilometers east of the McDermitt caldera lies the mid-Miocene Santa Rosa–Calico volcanic field, which includes rhyolites that erupted mostly effusively and which range in age from 16.7–15.4 Ma. The period of peak activity based on existing geochronological data appears to be from 16.0–16.4 Ma [15].

3.2.5. Juniper Mountain Complex (23 in Figure 4)

The Juniper Mountain complex lies in Idaho near the Oregon/Idaho state border, about 50 km northwest of the Santa Rosa–Calico field [79]. Rhyolite lavas here range from 14.5–13.5 Ma, and hence, we consider only the oldest rhyolite to be related to the basaltic input of the Columbia River Basalt during its main phase from ~17 to ~<16 Ma (see Section 4).

3.2.6. Silver City Range (22 in Figure 4)

The Silver City Range is located farther north along the Oregon/Idaho state border in Idaho. Rhyolite lavas yielded three ages spreading from the earliest Columbia River Rhyolites to the latest activity. These ages are 16.66 $\pm$ 0.08 Ma, 16.33 $\pm$ 0.12 Ma, and 14.21 $\pm$ 0.11 Ma [4].

3.2.7. Weiser Embayment Volcanic Field (21 in Figure 4)

Recent mapping around the Weiser Embayment in Idaho revealed the existence of a mid-Miocene volcanic field that also produced rhyolites. A capping ignimbrite yielded a U-Pb age zircon age of 16.394 $\pm$ 0.008 Ma [89]. Since it is a capping unit, stratigraphically lower rhyolites are expected to be slightly older.

3.2.8. Rhyolites of Bald Butte (32 in Figure 4), Drum Hill (32 in Figure 4), and Twenty Mile Creek (31 in Figure 4)

In their study of late Miocene to Pliocene rhyolites of the High Lava Plains of Oregon, Ford et al. [63] found three rhyolite centers to be mid-Miocene and hence to be older than rhyolite volcanism associated with the progressive age trend of the High Lava Plains (Figure 2A). Bald Butte (32 north) is 17.53 $\pm$ 0.08 Ma, and Drum Hill (32 south) is 17.30 $\pm$ 0.09 Ma (Figure 4). The rhyolite of Twenty Mile Creek [31] is 15.13 $\pm$ 0.08 Ma and is located in Oregon near the Oregon–Nevada–California state border (Figure 4). Compositions indicate they range from A-type to calc-alkaline in character, respectively [63].

3.2.9. Mid-Miocene Dacites of the Harney Basin (33, 34 in Figure 4)

MacLean [90] and Jordan et al. [39] determined that mid-Miocene dacite dome complexes are located along the periphery of the Harney Basin. Two of these dacite domes—Horsehead Mountain (33 in Figure 4), dated at 15.63 $\pm$ 0.03 Ma, and Little Juniper Mountain [58], dated at 15.65 $\pm$ 0.04 Ma—lie in the southwest corner of the Harney Basin [39]. Jackass Mountain (34 in Figure 4), located in the southeast corner of the Harney Basin, near the Dome E of South Fork (see Section 3.1.4, yielded an age of 15.34 $\pm$ 0.19 Ma [65].

4. Discussion

4.1. Distribution and Waxing and Waning of Columbia River Rhyolite Activity

Combining our data and the previous literature's data, we divide 17.5–14.5 Ma rhyolites associated with the Columbia River province into four age brackets (Table 2): 17.5–16.4 Ma, 16.3–15.9 Ma, 15.8–15.4 Ma, and 15.3–14.5 Ma. This approach is intended to focus on patterns in eruption ages, but volume considerations are discussed later. Although the ~32 rhyolite centers that erupted between 17.5 Ma and 14.5 Ma (Figure 4 and Table 2) vary in eruptive volumes, we emphasize the timing and location of these eruptions because these data are useful in tracking where large reservoirs of basalt magma must have resided in the crust as a heat and/or material source (see Section 4.3). These activity duration data are minima, as additional ages from centers with few ages could extend the activity period for each eruptive center. The four sub-ranges within the overall 17.5–14.5 Ma range were chosen because they each represent a critical period of activity; the 17.5–16.4 Ma range captures the earliest eruptive centers, two ranges of 400,000 year duration (16.3–15.9 Ma and 15.8–15.4 Ma) reflect the middle of the overall age range, and the 15.3–14.5 Ma captures the tail end of activity. The oldest episode of rhyolite eruptions has a wide footprint (Figure 11A), from the Drumhill–Bald Butte center (32 in Figure 4) in the southwest to Unity [3] and the Weiser Embayment [21] in the north; to Silver City [22] along the central eastern flank; and to the axis of Hawks Valley, High Rock, McDermitt, and Santa Rosa–Calico centers straddling the Oregon–Nevada state border. The only center that falls somewhere in the middle of the area defined by the others is the Dome E of South Fork [16] (Figures 4 and 11). All of the larger centers stayed active into the 16.3–15.9 Ma range, when numerous other rhyolite eruptions commenced. Notably, eruptive activity within the northern (43–45° N) and southern (41–43° N) areas (cf. Table 2) remains nearly consistent over time. However, in the north, many new centers in different locations become active over time, while younger activity in the south is largely confined to the same centers that were previously active. Coble and Mahood [17] have noted that overall, centers in the High Rock caldera complex become slightly younger towards the SSW. Lastly, fewer rhyolites erupted in the last age range, but they are still within the same large footprint. We included the Jarbidge rhyolite [23] in these maps, but note that prior workers considered activity in that locality to be associated with propagating rifting rather than the CRBG (e.g., [23]). Regardless, there appears to be no south-to-north progression of rhyolite volcanic activity from 17.5–14.5 Ma (Figure 11) (cf. [17,39]). Rather, rhyolite eruptive activity appears to have waxed and waned across the entire footprint of 17.5–14.5 Ma volcanism. This is also evident if we use three subequal time slices instead of four (Figure 11E). The noted south-to-north progression was based on incomplete and locally inaccurate ages. With our updated and expanded geochronologic dataset, a more likely footprint of co-CRBG rhyolite activity emerges. Additionally, these data highlight the well-defined northern, western, and eastern spatial termination of rhyolite volcanism in this period. The southern terminus is more diffuse as there are 16–15 Ma rhyolites associated with ore deposits farther south in Nevada (36 in Figure 4) (cf. [91,92]). It is less clear whether those are associated with flood basalt magmatism or with Basin and Range extension. Even if we include these, the general conclusions reached are the same.

It is also important to note that silicic volcanism impacted the area of the Columbia River Rhyolites prior the Columbia River rhyolite flare-up. During the late Oligocene, mainly around 22–25 Ma, eastern Oregon silicic volcanism typically consisted of more dacite and less rhyolite [80,93–97]. This episode of volcanism was revealed only very recently in certainly places. Furthermore, these older volcanic rocks are only exposed along deep-seated fault scarps and at other local uplifts. Notably, this suggests a hiatus in silicic volcanism of about 5–8 million years before initiation of Columbia River rhyolite volcanism, and this indicates that prior silicic volcanism was also widespread and typically calc-alkaline in character.

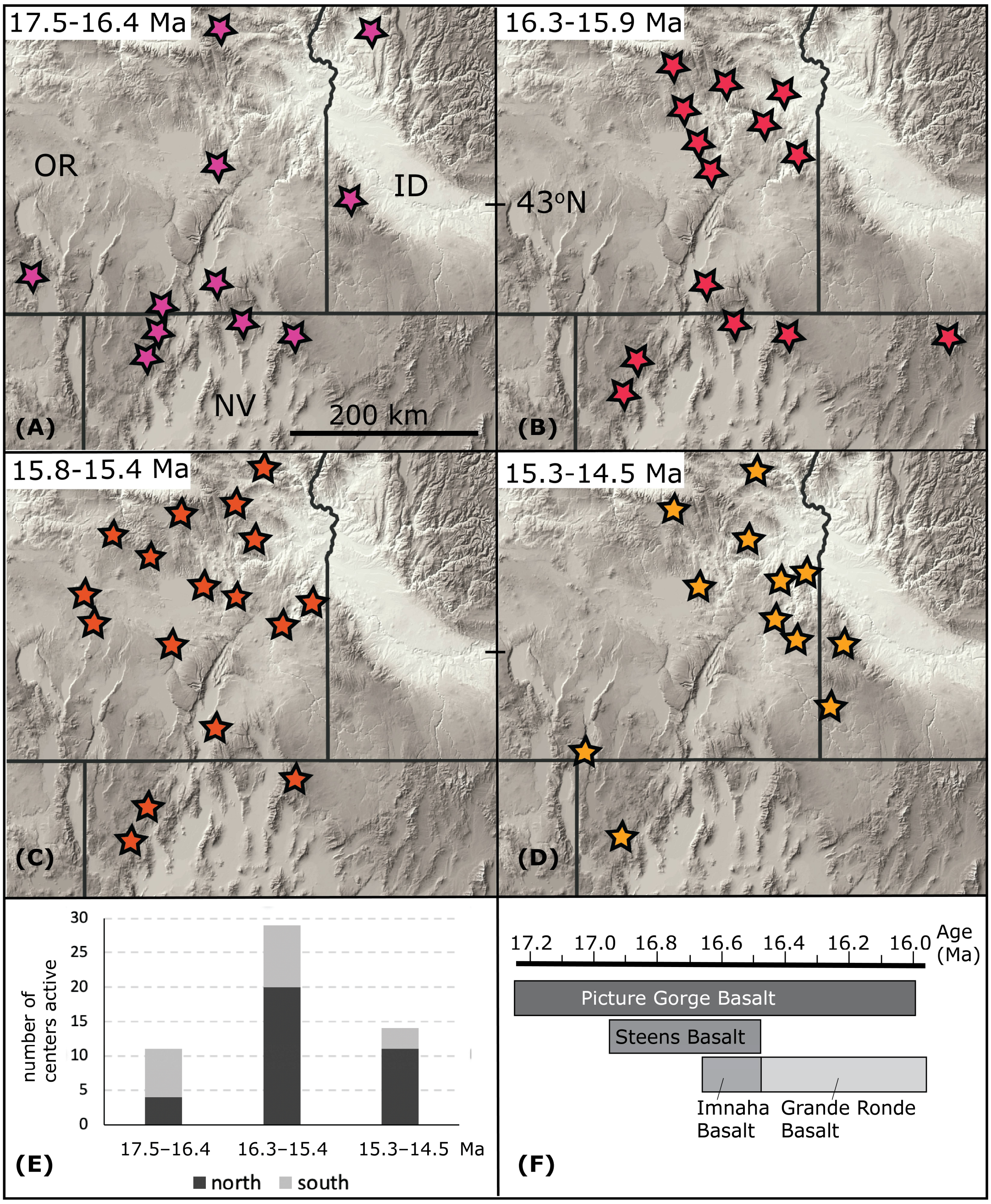

Figure 11. (**A**–**D**): Temporal and spatial distribution of rhyolite centers across four time windows; (**E**) histogram of active centers, north: 43–45° N, south: 41–43° N; and (**F**) ages of main phase CRBG flood basalt units (cf. [98]). Diagrams show broad distribution of rhyolite centers at the onset of activity from 17.5–16.4 Ma, intense and widespread rhyolite magmatism during 16.3–15.4 Ma across the province, and waning activity from 15.3–14.5 Ma. OR: Oregon, ID: Idaho, NV: Nevada.

4.2. Mid-Miocene Rhyolites in Context to CRBG

Radiometric ages of rhyolites of this study and previously published data range from 17.5–14.5 Ma. Main phase CRBG magmas—consisting of Steens Basalt, Imnaha, Picture Gorge (PGB), and Grand Ronde Basalt units—account for 92% of all CRBG volume [5]. Lavas of this main phase CRBG erupted over less than 1–1.5 m.y., starting at ~16.9 Ma [12,99]. The newest age data suggest that the PGB started to erupt at ~17.2 Ma [100], hence it appears to be the earliest-erupting CRBG. More importantly, this indicates that the onsets of PGB and Steens Basalt were essentially synchronous, as the currently oldest known age of Steens Basalt is 16.97 ± 0.06 Ma [99]. The most voluminous member of the CRBG is the Grand Ronde Basalt, accounting for 75% of all CRBG magmas [101]. Chronology from [1] suggesting that Grande Ronde Basalt eruptions took place from ~16–15.6 Ma has been questioned (cf. [27]); on the other hand, the [12,102] chronologies indicate eruptions began at 16.54 Ma and ended at 15.95 Ma in paleomagnetic chron C5Cn.1n. Consequently, waxing rhyolite activity largely coincided with Steens Basalt and PGB as well as Imnaha Basalt, while eruption of the main pulse of rhyolites coincided with Grande Ronde Basalt volcanism but outlasted it by ~400 ky.

Direct stratigraphic evidence for contemporaneity of CRBG volcanism and rhyolites is within areas where CRBG units are intercalated with rhyolites. This area includes (1) the greater Malheur River Gorge area (Figure 3), where Grande Ronde Basalt is intercalated with rhyolites overlying older CRBG units (e.g., [16,70,98], and (2) peripheral areas in which units of the Dinner Creek Tuff are intercalated into Grande Ronde Basalt at Rattlesnake Road [18], north of Baker City, and along the Oregon/Idaho state border east of Baker City (Figure 3). Additionally, several other ignimbrite units emplaced farther south are intercalated with Steens Basalt [103]. Evidence for contemporaneousness and for overlapping locations of late Grande Ronde Basalt and rhyolite magmas are found in ignimbrites that contain mafic glassy fragments of late Grande Ronde compositions. These ignimbrites include some Dinner Creek Tuff units [19], the Wildcat Creek Tuff [81] and the tuff of Buchanan (Figure 9). Residence of Grande Ronde Basalt magmas beneath rhyolites is also inferred from petrological evidence in the case of the upper Littlefield Rhyolite [71]. In late Grande Ronde Basalt magmas, we also include Fe-rich andesites (icelandites) that show direct lineages to Grande Ronde magmas (Figure 9) ([19,26,71,81]. All these data are corroborated by late Grande Ronde eruption sites that are within the same locations [7,71]). This area largely overlaps the area previously postulated to have been the location of a general storage site for CRBG magmas (Figure 12D) [11], and it coincides well with what is inferred from the distribution of Columbia River Rhyolites (see above).

4.3. Consequences of Arrival, Storage, and Dispersal of Columbia River Basalt Magmas

End-member models for how rhyolites can be generated range from partial melting of the crust to fractional crystallization of mafic magmas. In the former model, basalt magmas provide heat to induce partial melting, and in the latter model, basaltic magmas provide the source material for generating rhyolites by crystal fractionation. Though the specific details of each model differ, basalt magmas are involved in the petrogenesis of rhyolites in both models, and therefore, rhyolites are clear indicators of where a thermal pulse originating from the mantle is delivered to the crust via injection of basalt, irrespective of the details of rhyolite petrogenesis (e.g., [30]). Some incubation time from basalt heat input to generation of rhyolites can be assumed [104], although recent thermal models suggest that this period can be very short. Rhyolites of continental flood basalt provinces offer an alternative and complementary perspective on the temporal evolution of the arrival, dispersion, and storage of flood basalt magmas. Rhyolite magmas may be produced in the crust but fail to erupt, or they may mix with basalt to produce intermediate magmas. Thus, documenting rhyolite magmatism can only be based on rhyolite exposures on the surface, and these rhyolites are a minimum expression. Additionally, erosion and coverage by younger rocks can reduce the original surface extent of rhyolites. Considering all these factors that influence eruptive area and volume estimates, we use the details of rhyolite activity through time (Figure 10) to infer basalt activity at depth. Lastly, it should be noted that basalt magmas at depth may interact with the crust in such a way that no rhyolite magmas are generated, but instead, intermediate magmas are produced through fractional crystallization or through open system assimilation and contamination processes.

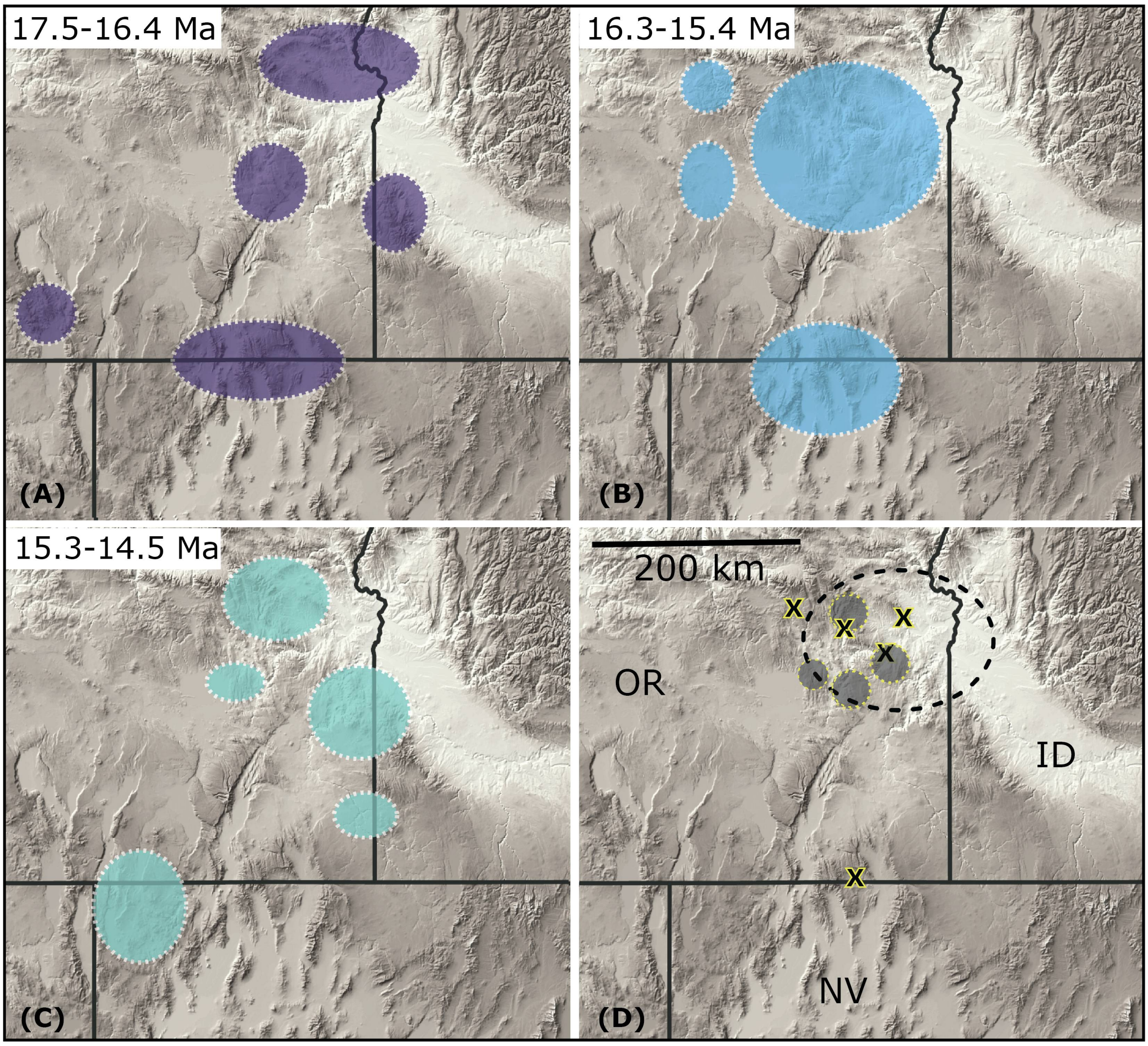

Figure 12. Inferred flood basalt intrusive focal points based on distribution and ages of rhyolites of Figure 11, see text for discussion and age of main phase CRBG depicted in Figure 11F. (**A**) Early focal points coeval with early CRB eruptions of PGB, Steens, and lower Imnaha Basalt; (**B**) main focal points of extensive crustal reservoirs associated with the voluminous Grande Ronde Basalt eruptions and later PGB; (**C**) crustal reservoirs emplaced during the waning phases of CRB magmatism; (**D**) known dike swarms and inferred locations of Grande Ronde Basalt reservoirs (gray circles), eruption sites of Hunter Creek Basalt and icelandites (X), and inferred general storage area (dashed oval) of [11] see text for discussion. OR: Oregon, ID: Idaho, NV: Nevada.

Rhyolites associated with the CRBG first erupted from 17.5 Ma to ~16.4 Ma over a wide area in eastern Oregon, western Idaho, and northern Nevada, indicating basalt magmas at depth. Mafic CRBG eruptions began with the 17.2 Ma Picture Gorge Basalt [100] of northeastern Oregon and the 17.0 Ma Steens Basalt [86] in the south, coinciding with rhyolite eruptions in the north, at the Unity area, in the west along the eastern Harney Basin, and in the south along the Nevada–Oregon border (Figures 11 and 12). Rhyolites with slightly younger ages of 16.7 Ma and 16.4 Ma around Silver City and Weiser could be associated with the initial pulse of Imnaha magmas, generally thought to be 16.7–16.4 Ma (Figures 11 and 12). There may be an even earlier basalt pulse predating this given the 17.53–17.30 Ma ages of Bald Butte and Drum Hill [62] (Figure 12). In any case, the distribution of rhyolite centers indicates that flood basalt magmas ascended from the mantle at approximately the same time across the entire region.

Based on the volume and number of active centers, the 16.3–15.9 Ma and 15.8–15.4 Ma subranges indicate that rhyolite volcanism was most intense during this time (Figure 11 and Table 2). This phase correlates well with the later PGB (cf. [98]) and particularly well with the voluminous Grande Ronde Basalt, which is ~16.3 to 15.9 Ma. Thus, magma reservoirs hosting these mafic magmas must have been widespread in the crust below those rhyolite centers (Figure 12 and Section 4.2). Additionally, icelandites are not uncommon in this time window, occurring both as commingled icelandite–rhyolite ignimbrite eruptions and as distinct mafic lavas and vent deposits (Figure 9). These icelandite eruption locations coincide with much of the northern sector rhyolites, and they are also reported from southern sector centers (e.g., [26]). Icelandites suggest protracted magmatic evolution (cf. [105]), and this can serve as evidence that longer lived crustal reservoirs existed during this time range.

Although the last rhyolites from 15.3–14.5 Ma are younger than the main phase units of the CRBG, basalt magmas are inferred at depth in this time frame. Some of the rhyolites of this time window are observed underlying or are intercalated with mafic lavas. Such is the case with units of the Strawberry Volcanics [53,70] and where the Oywhee Basalt overlies the 14.7 Ma "Dam" rhyolite at the Owyhee reservoir. Interestingly, these mafic lavas are either tholeiitic basalt or relatively evolved calc-alkaline basaltic andesite to andesite lavas, where magmatic evolution is driven by open system processes (e.g., [70]). The evolved mafic lavas mark a distinct younger phase of calc-alkaline magmatism (14.2–10.0 Ma) in eastern Oregon (Stage 5 of [71]) after the CRBG and subsequent tholeiites (14.4–13.3 Ma) [71].

The well-defined northern, western, and eastern spatial extents of 17.5–14.5 Ma rhyolite volcanism delimit the area in which basalt magmas resided long enough in the crust to generate rhyolite. In turn, this suggests that CRBG dikes of the Chief Joseph and Monument dike swarms located beyond these limits were not fed by magmas from reservoirs located below the dikes but rather that they were fed laterally from reservoirs residing within the footprint of the rhyolite distribution (cf. Figure 1).

4.4. Consideration of Volume for Inferences of the Vigor of Basalt Magmatism

A number of researchers have pointed to volume of rhyolite being an important parameter for inferences about basalt magmatism at depth (e.g., [46]). The argument is that the volume of rhyolite erupted correlates with the basalt volume at depth, implying that where rhyolites are most voluminous, basalt magmatism is most voluminous. This statement has been used to argue that intrusion of CRBG magmas along the Oregon-Nevada border was much more significant than within the area of the northern sector of co-CRBG rhyolites.

First, the area of rhyolites exposed represents what has withstood post-emplacement erosion and what was not obscured by later deposition. Such deposition includes but is not limited to the abundant post-rhyolite eruptive activity in the northern sector (cf., [46]). However, to address the more notable challenge to direct correlation of rhyolite and basalt volumes, it is critical to remember that the volume of rhyolite produced in partial melting strongly depends on the composition of the material that is melting. Mafic protoliths will produce considerably less rhyolite than felsic protoliths at the same conditions (e.g., [106]). It has long been known that the area in which rhyolites of the northern sector were emplaced is underlain by a variety of terrains that were accreted onto the North American continent during the Mesozoic. In contrast, all very voluminous rhyolite centers of the southern sector are underlain by more felsic and thicker crust (e.g., [107,108]). Furthermore, as mentioned above, rhyolites generated at depth may have not persisted as rhyolites, as they may have mixed with basalt or experienced basalt–crust interaction that generated non-felsic melts. For example, virtually all Grand Ronde Basalt magmas are not basalt but basaltic andesite, requiring 9% to 56% of crust to arrive at the observed isotopic endmember compositions of the Grande Ronde Basalt [27]. The estimated volume of the Grande Ronde Basalt is 150,400 km^3 [27], and hence if even 10% of crust was consumed during its generation, this is a substantial amount of potential melt. This discussion clearly indicates that using solely rhyolite volume considerations will inaccurately predict relative basalt magma volumes at depth, especially those of such a wide and lithologically diverse area as discussed here.

4.5. Implications for the Age-Progressive Snake River Plain–Yellowstone Rhyolite Trend and for the Pre-CRBG Hotspot Track

The traditional starting point of age-progressive Snake River Plain–Yellowstone trend is considered to be ~16.5 Ma at the McDermitt volcanic field, followed by the ~14 Ma Owyhee Humboldt volcanic field, the 12 Ma Bruneau-Jarbidge center, and others, culminating at present day Yellowstone (Figures 1 and 13) [38]. This has not fundamentally changed in modern research (cf., [50]). The footprint of waning activity (i.e., 15.3–14.5 Ma; see Figure 11D) among Columbia River Rhyolites does not include the McDermitt nor the Santa Rosa–Calico volcanic centers as being active, but it does include rhyolite centers farther north—the southernmost of which are Birch Creek, Dam, Dry Creek, Silver City, and Juniper Mountain—and centers in the far southwest of the rhyolite province (Figure 11D). Juniper Mountain is the closest center to the alleged Snake River Plain hot spot track that was active between 14.5 Ma and 13.5 Ma (Figure 13) [109].

Most other $\leq$ 12.5 Ma centers potentially related to the Snake River Plain are located along the Oregon–Idaho state border in a corridor from Mahogany Mountain to the Idaho–Nevada state border to the Bruneau-Jarbidge center (Figure 13). Rhyolites of this age are those of the Idaho Front, including the voluminous Jump Creek Rhyolite [4,110], and they overlap the eastern flank of the MM-TFrf. Very few precise or even older ages exist for rhyolites south of Juniper Mountain. The only two published ages from rhyolites of this area are from the Circle Creek rhyolite, ranging from 12–11 Ma [111]. The Circle Creek rhyolite is located directly at the Idaho–Nevada state border and is part of the Owyhee Humboldt volcanic field. The Juniper Mountain and the Santa Rosa–Calico fields are sometimes included in the Owyhee Humboldt volcanic field as well, hence the depicted activity span for the Owyhee Humboldt field varies, such as 14.5–12.8 Ma reported by [46] and 15.9–12.8 Ma stated in [112]. It appears that the main area covered by the Owyhee Humboldt field is poorly studied, with little published geochronologic data. Historically, most ages cited for this field were acquired from units within the area of Juniper Mountain that lies at the very northern end of the rather large Owyhee Humboldt volcanic field (cf., [38,109]). This is indeed important when we revisit the alleged Snake River Plain hotspot track (e.g., [38,50]) that was largely formulated without knowing the true ages and age distribution of the northern sector rhyolites described here. Age distribution patterns discussed here suggest that McDermitt is likely not the starting point of the Snake River Plain trend but rather that it belongs to the early- to middle-aged Columbia River Rhyolites. Based on age of activity (Figure 11), this appears to also be the case for rhyolites of the Santa Rosa–Calico volcanic field, rhyolite centers in the northeast portion of the High Rock Caldera complex, and the northern McDermitt volcanic complex, so the starting point of the Snake River Plain trend remains in question. True locations of rhyolite activity $\leq$ 12.5 Ma are better aligned with an initial eastward migration that coincides with "path B" of [37] (see Figure 2B) first mentioned in [49]. This eastward migration may start after a brief hiatus in rhyolite activity of ~1 m.y. Interestingly, if not for rhyolites of the Juniper Mountain center, this hiatus would be 14.5–12.5 Ma, similarly to the one observed in the westward-migrating High Lava Plains rhyolites (cf., [34]). Returning to the hotspot track discussion, "path B" was considered unlike a hot spot track as field data, such as the noted south-to-north basalt and rhyolite migration trends, implied a plume axis farther south ([37] and discussion therein). Additionally, path B does not parallel the direction of plate motion, which has been suggested to be due to complications of plume–cratonic lithosphere interactions [49]. Plate motion that causes a linear chain of volcanic centers is only expected if we treat the thermal anomaly that intercepts the crust (i.e., basalt from the mantle) as a stable point source. Columbia River Rhyolites clearly indicate that the thermal pulse was not a simple point source until at least 14.5 Ma and possibly not until after ~12 Ma. From this, we propose that true plate motion dictated and focused rhyolite activity (Yellowstone track) starts with the Bruneau-Jarbidge center at ~12 Ma and not at the McDermitt center or any other center nearby.

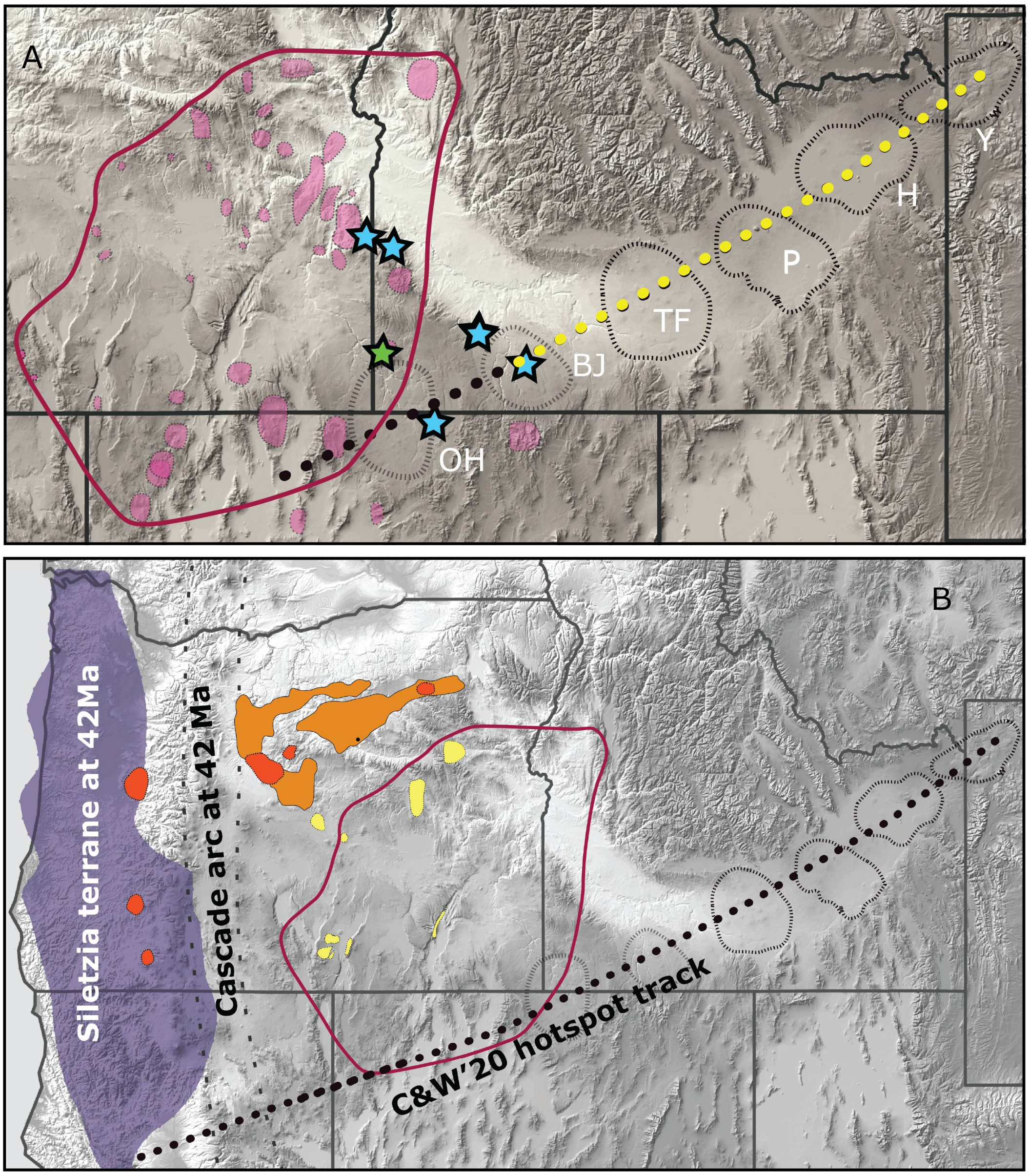

Figure 13. (**A**) Columbia River Rhyolites (red) and younger centers discussed in text. Green star indicates activity span of 14.5 to 13.5 Ma for Juniper Mountain rhyolites. Blue stars indicate next-younger eastward rhyolite centers, starting at 12.5 Ma, including (from N to S) Jump-Creek rhyolite and other Idaho Front rhyolites, Jack Creek center, Bruneau-Jarbidge (BJ) center, and Circle Creek rhyolite. No other ages are published for the Owyhee Humboldt volcanic center (OH). Location of Twin Falls (TF), Picabo (P), Heise (H), Yellowstone (Y), and axis of age progressive rhyolite trend (thick dotted line) are from [50]. Extent and location for OH and BJ centers from [83]. Yellow SRP hotspot track is a track that is proposed here (see Section 4). (**B**): Expanded view with entire hotspot track, location of the Siletzia terrane, and position of ancestral Cascades at 42 and 40 Ma respectively, all taken from [50]. Widespread silicic rocks of the Oligocene John Day Formation (orange) and Oligocene calderas (red) from [96]. Other occurrences of Oligocene silicic rocks show in yellow (e.g., [97] and references therein; [93,94]).

We now consider a recent model that links the CRBG to the Eocene flood basalts of the Siletzia plume via a hot spot track. In this model, magmas of the CRBG are caused by a secondary upwelling of mantle material and are not caused by the arrival of a plume head [50,51]. A significant component of this model is the ~30 m.y. age gap between 56–41 Ma Siletzia [51] eruptions and 17.5–14.5 Ma eruptions of the CRBG. The nature and migration of volcanic activity from inception of the Siletzia plume to CRBG volcanism is in question. Can migration be traced as a narrow "hotspot track", as discussed for the Snake River Plan trend, or could it be a broad zone? Camp and Wells [50] propose a narrow hotspot track, yet the distribution of Fe-rich, A-type rhyolites and other calc-alkaline rhyolites active between 35 to 20 Ma suggests a broad migration (cf. [96,97] and references therein), if any migration at all (Figure 13). Hence, we suggest that classical hotspot track systematics like those observed in the ocean basins should not be used as a critical interpretation framework for continental flood basalts and ensuing volcanism, as discussed here for the Pacific Northwest.

5. Conclusions

We investigated numerous understudied mid-Miocene rhyolite centers in eastern Oregon. Combining our new distribution and ages of rhyolite centers with those discussed in previous literature, we consider rhyolites spanning from 17.5–14.5 Ma of eastern Oregon, northern Nevada, and western Idaho to be a direct response of flood basalts of the Columbia River Basalt Group, and we collectively categorize them as Columbia River Rhyolites. The spatiotemporal patterns of Columbia River Rhyolites have implications for arrival, location, and dispersion of flood basalt magmas in the crust. The period from 17.5–16.4 Ma was the waxing phase of rhyolite activity, and the period from 15.3–14.5 Ma was the waning phase. Most rhyolite centers were active between 16.3–15.9 Ma and 15.8–15.4 Ma. The location of centers within the waxing phase imply arrival of CRBG magmas across the distribution area of rhyolites. These rhyolites are thought to correspond to the thermal pulses correlated to the arrival of Picture Gorge Basalt and Picture-Gorge-Basalt-like magmas of the Imnaha Basalt in the north and with Steens Basalt magmas in the south. The 16.3–15.9 Ma phase of prominent rhyolite volcanism corresponds to Grande Ronde Basalt and evolved PGB and Steens Basalt. The 15.8–15.4 Ma phase of eruptive activity slightly postdated the aforementioned flood basalts but are contemporaneous with icelanditic magmas that evolved from flood basalts. Centers within the waning phase span the areal distribution of earlier waxing phase. This suggests the following:

1. There is no south-to-north age progression within the rhyolites, and the perceived progression was a result of an incomplete geochronological dataset of regional rhyolites. Consequently, the age progression interpreted in main CRBG units from south to north may simply be a function of where these eruptions occurred and not where mantle magmas were delivered.
2. The rhyolite flare-up associated with CRBG volcanism covers a broad area and is focused significantly north of the McDermitt eruptive center and other earlier centers along the Oregon–Nevada state border.
3. Arrival of the thermal anomaly associated with flood basalts is essentially "instantaneous" across a circular area of 300–400 km, which seems to be best matched with the arrival of a mantle upwelling, irrespective of whether it was deep- or shallow-sourced.
4. Distribution of rhyolites is well delimited in the west, north, and east, and this distribution likely reflects the extent of flood basalt reservoirs in the crust. Consequently, CRBG dikes of the Chief Joseph and Monument dike swarms located beyond these limits were likely not fed by magmas from crustal reservoirs located below the dikes. Rather, these swarms are keel dikes that were likely fed laterally from reservoirs residing within the footprint of the rhyolite distribution.
5. The long-held view of McDermitt (and other early centers along the Oregon–Nevada state border) as the start of the age-progressive Snake River Plain trend (and which has been interpreted as hotspot track) must be revisited. Young Columbia River Rhyolites and younger centers suggest a more diffuse west–east migration starting farther north rather than a northeast migration from the McDermitt center. We suggest true age-

progressive rhyolite volcanism paralleling plate motion of the North America plate started at the Bruneau-Jarbidge center from ~12 Ma onward towards Yellowstone.

Supplementary Materials: The following are available online at https://www.mdpi.com/article/10.3390/geosciences13020046/s1.

Author Contributions: Writing—original draft preparation, M.J.S.; writing—review and editing, M.J.S., V.M.S., W.M., M.L.F. and M.H.; funding acquisition, M.J.S. All authors have read and agreed to the published version of the manuscript.

Funding: This research was funded by the National Science Foundation grant EAR-1220676 to M.J. Streck.

Data Availability Statement: The data are available in the Supplementary Materials.

Acknowledgments: The first author acknowledges the numerous theses that this study is largely based on and thanks the following graduate students who contributed: Cassandra Black, Melissa Carley, Matthew Cruz, Chanel Dvorak (now Thieme), Teresa Hanna, Emily Hess, Robert Jackson, Adam Large, Phil Marcy, Hillary Sales, Arron Steiner, Brian Webb, and Brianna Young. We also acknowledge the detailed journal reviews of Eric Christiansen and two other anonymous reviewers that helped to improve this contribution. Publication of this article in an open access journal was funded by the Portland State University Library's Open Access Fund.

Conflicts of Interest: The authors declare no conflict of interest.

References

1. White, R.S.; McKenzie, D. Magmatism at rift zones: The generation of volcanic continental margins and flood basalts. *J. Geophys. Res.* **1989**, *94*, 7685–7729. [CrossRef]
2. White, R.S.; McKenzie, D. Mantle plumes and flood basalts. *J. Geophys. Res.* **1995**, *100*, 17543–17585. [CrossRef]
3. Barry, T.L.; Kelley, S.P.; Reidel, S.P.; Camp, V.E.; Self, S.; Jarboe, N.A.; Duncan, R.A.; Renne, P.R. Eruption chronology of the Columbia River Basalt Group. In *The Columbia River Flood Basalt Province: Geological Society of America Special Paper*; Reidel, S.P., Camp, V.E., Ross, M.E., Wolff, J.A., Martin, B.S., Tolan, T.L., Wells, R.E., Eds.; Geological Society of America: Boulder, CO, USA, 2013; Volume 497, pp. 45–66.
4. Bonnichsen, B.; Leeman, W.P.; Honjo, N.; McIntosh, W.C.; Godchaux, M.M. Miocene silicic volcanism in southwestern Idaho: Geochronology, geochemistry and evolution of the central Snake River Plain. *Bull. Volcanol.* **2008**, *70*, 315–342. [CrossRef]
5. Camp, V.E.; Ross, M.E. Mantle dynamics and genesis of mafic magmatism in the intermontate Pacific Northwest. *J. Geophys. Res.* **2004**, *109*.
6. Camp, V.E.; Ross, M.E.; Duncan, R.A.; Jarboe, N.A.; Coe, R.S.; Hanan, B.B.; Johnson, J.A. The Steens Basalt: Earliest lavas of the Columbia River Basalt Group. In *The Columbia River Flood Basalt Province: Geological Society of America Special Paper*; Reidel, S.P., Camp, V.E., Ross, M.E., Wolff, J.A., Martin, B.S., Tolan, T.L., Wells, R.E., Eds.; Geological Society of America: Boulder, CO, USA, 2013; Volume 497, pp. 87–116.
7. Ferns, M.L.; McClaughry, J.D. Stratigraphy and volcanic evolution of the middle Miocene to Pliocene La Grande–Owyhee eruptive axis in eastern Oregon. In *The Columbia River Flood Basalt Province: Geological Society of America Special Paper*; Reidel, S.P., Camp, V.E., Ross, M.E., Wolff, J.A., Martin, B.S., Tolan, T.L., Wells, R.E., Eds.; Geological Society of America: Boulder, CO, USA, 2013; Volume 497, pp. 401–427.
8. Hooper, P.R.; Binger, G.B.; Lees, K.R. Ages of the Steens and Columbia River flood basalts and their relationship to extension related calc-alkalic volcanism in eastern Oregon. *Geol. Soc. Am. Bull.* **2002**, *114*, 43–50. [CrossRef]
9. Hooper, P.R.; Camp, V.E.; Reidel, S.P.; Ross, M.E. The origin of the Columbia River Flood Basalt province: Plume versus nonplume models. *GSA Spec. Pap.* **2007**, *430*, 635–668.
10. Sawlan, M.; Hagstrum, J.T.; Wells, R.E. Geologic Mapping and Paired Geochemicalpaleomagnetic Sampling of Reference Sections in the Grande Ronde Basalt: An Example from the Bingen Section, Columbia River Gorge, Washington. In Proceedings of the Fall Meeting 2011, San Francisco, CA, USA, 5–9 December 2011; abstract #V13C-2605. American Geophysical Union: Washington, DC, USA, 2011.
11. Wolff, J.A.; Ramos, F.C.; Hart, G.L.; Patterson, J.D.; Brandon, A.D. Columbia River flood basalts from a centralized crustal magmatic system. *Nat. Geosci.* **2008**, *1*, 177–180. [CrossRef]
12. Jarboe, N.A.; Coe, R.S.; Renne, P.R.; Glen, J.M.G. The age of the Steens reversal and the Columbia River Basalt Group. *Chem. Geol.* **2010**, *274*, 158–168. [CrossRef]
13. Fiebelkorn, R.B.; Walker, G.W.; MacLeod, N.S.; McKee, E.H.; Smith, J.G. *Index to K-Ar Age Determinations for the State of Oregon*; U.S. Geological Survey Open-File Report 82-0596; U.S. Geological Survey: Baltimore, MD, USA, 1982; 42p.

14. Vander Meulen, D.B. *Intracaldera Tuffs and Central-Vent Intrusion of the Mahogany Mountain Caldera, Eastern Oregon*; U.S. Geological Survey Open-File Report 89-77; U.S. Geological Survey: Baltimore, MD, USA, 1989.
15. Brueseke, M.E.; Hart, W.K.; Heizler, M.T. Diverse mid-Miocene silicic volcanism associated with the Yellowstone–Newberry thermal anomaly. *Bull. Volcanol.* **2008**, *70*, 343–360. [CrossRef]
16. Camp, V.E.; Ross, M.E.; Hanson, W.E. Genesis of flood basalts and Basin and Range rocks from Steens Mountain to the Malheur River Gorge, Oregon. *Geol. Soc. Am. Bull.* **2003**, *115*, 105–128. [CrossRef]
17. Matthew, A.; Mahood, G.A. Initial impingement of the Yellowstone plume located by widespread silicic volcanism contemporaneous with Columbia River flood basalts. *Geology* **2012**, *40*, 655–658.
18. Cummings, M.L.; Evans, J.G.; Ferns, M.L.; Lees, K.R. Stratigraphic and structural evolution of the middle Miocene syn-volcanic Oregon-Idaho graben. *Geol. Soc. Am. Bull.* **2000**, *112*, 668–682. [CrossRef]
19. Streck, M.J.; Ferns, M.L.; McIntosh, W. Large, persistent rhyolitic magma reservoirs above Columbia River Basalt storage sites: The Dinner Creek Tuff Eruptive Center, eastern Oregon. *Geosphere* **2015**, *11*, 226–235. [CrossRef]
20. Bryan, S.E.; Riley, T.R.; Jerram, D.A.; Stephens, C.J.; Leat, P.T. Silicic volcanism: An undervalued component of the large igneous provinces and volcanic rifted margins. *Geol. Soc. Am. Spec. Pap.* **2002**, *362*, 99–120.
21. Bryan, S.E.; Peate, I.U.; Peate, D.W.; Self, S.; Jerram, D.A.; Mawby, M.R.; Marsh, J.S.; Miller, J.A. The largest volcanic eruptions on Earth. *Earth Sci. Rev.* **2010**, *102*, 207–229. [CrossRef]
22. Benson, T.R.; Mahood, G.A.; Grove, M. Geology and $^{40}Ar/^{39}Ar$ geochronology of the middle Miocene McDermitt volcanic field, Oregon and Nevada: Silicic volcanism associated with propagating flood basalt dikes at initiation of the Yellowstone hotspot. *Geol. Soc. Am. Bull.* **2017**, *129*, 1027–1051. [CrossRef]
23. Brueseke, M.E.; Callicoat, J.S.; Hames, W.; Larson, P.B. Mid-Miocene rhyolite volcanism in northeastern Nevada: The Jarbidge Rhhyolite and its relationship to the Cenozoic evolution of the northern Great Basin (USA). *Geol. Soc. Am. Bull.* **2014**, *126*, 1047–1067. [CrossRef]
24. Coble, M.A.; Mahood, G.A. New geologic evidence for additional 16.5–15.5 Ma silicic calderas in northwest Nevada related to initial impingement of the Yellowstone hotspot. Collapse Calderas Workshop. *IOP Conf. Ser. Earth Environ. Sci.* **2008**, *3*, 012002. [CrossRef]
25. Henry, C.D.; Castor, S.B.; McIntosh, W.C.; Heizler, M.T.; Cuney, M.; Chemillac, R. Timing of Oldest Steens Basalt Magmatism from Precise Dating of Silicic Volcanic Rocks, McDermitt Caldera and Northwest Nevada Volcanic Field. In Proceedings of the Fall Meeting 2006, Boston, MA, USA, 27 November–3 December 2006; no. abstract #V44C-08. American Geophysical Union: Washington, DC, USA, 2006.
26. Henry, C.D.; Castor, S.B.; Starkel, W.A.; Ellis, B.S.; Wolff, J.A.; Heizler, M.T.; McIntosh, W.C. *The McDermitt Caldera, NV-OR, USA: Geologic Mapping, Volcanology, Mineralization, and High Precision 40Ar/39Ar Dating of Early Yellowstone Hotspot Magmatism*; Fall Meeting 2012 abstract #V33B-2850; American Geophysical Union: Washington, DC, USA, 2012.
27. Wolff, J.A.; Ramos, F.C. Source materials for the main phase of the Columbia River Basalt Group: Geochemical evidence and implications for magma storage and transport. In *The Columbia River Flood Basalt Province: Geological Society of America Special Paper*; Reidel, S.P., Camp, V.E., Ross, M.E., Wolff, J.A., Martin, B.S., Tolan, T.L., Wells, R.E., Eds.; Geological Society of America: Boulder, CO, USA, 2013; Volume 497, pp. 273–291. [CrossRef]
28. Ernst, R.E.; Buchan, K.L. Giant radiating dyke swarms: Their use in identifying preMesozoic Large Igneous Provinces and mantle plumes. In *Large Igneous Provinces: Continental, Oceanic and Planetary Flood Volansim*; Mahoney, J.J., Coffin, M.F., Eds.; Geophys Monograph, SEG Library: Houston, TX, USA, 1997; Volume 100, pp. 297–333.
29. Ernst, R.E.; Liikane, D.A.; Jowitt, S.M.; Buchan, K.L.; Blanchard, J.A. A new plumbing system framework for mantle plume-related continental Large Igneous Provinces and their mafic-ultramafic intrusions. *J. Volcanol. Geotherm. Res.* **2019**, *384*, 75–84. [CrossRef]
30. Johnson, C.M. Large-scale formation and lithospheric modification beneath middle to late Cenozoic calderas and volcanic fields, western North America. *J. Geophys. Res.* **1991**, *96*, 1348513507.
31. Christiansen, R.L.; Foulger, G.R.; Evans, J.R. Upper-mantle origin of the Yellowstone hotspot. *Geol. Soc. Bull.* **2002**, *114*, 1245–1256. [CrossRef]
32. Fouch, M.J. The Yellowstone Hotspot: Plume or Not? *Geology* **2012**, *40*, 479–480. [CrossRef]
33. Liu, L.; Stegman, D.R. Origin of the Columbia River flood basalt controlled by propagating rupture of the Farallon slab. *Nature* **2012**, *482*, 386–390. [CrossRef]
34. Swenton, V.M.; Streck, M.J.; Miggins, D.P.; McIntosh, W.C. Filling critical gaps in the space-time record of High Lava Plains and co-Columbia River Basalt Group rhyolite volcanism. *GSA Bull.* **2022**. [CrossRef]
35. Pierce, K.L.; Morgan, L.A. Is the track of the Yellowstone hotspot driven by a deep mantle plume?—Review of volcanism, faulting, and uplift in light of new data. *J. Volcanol. Geotherm. Res.* **2009**, *188*, 1–25. [CrossRef]
36. Glen, J.G.; Ponce, D.A. Large-scale fractures related to inception of the Yellowstone hotspot. *Geology* **2002**, *30*, 647–650. [CrossRef]
37. Camp, V.E. *Origin of Columbia River Basalt: Passive Rise of Shallow Mantle, or Active Upwelling of a Deep-Mantle Plume? In the Columbia River Flood Basalt Province: Geological Society of America Special Paper*; Reidel, S.P., Camp, V.E., Ross, M.E., Wolff, J.A., Martin, B.S., Tolan, T.L., Wells, R.E., Eds.; Geological Society of America: Boulder, CO, USA, 2013; Volume 497, pp. 181–199.
38. Pierce, K.L.; Morgan, L.A. The track of the Yellowstone hot spot: Volcanism, faulting, and uplift. *Geol. Soc. Am. Mem* **1992**, *179*, 1–52.

39. Jordan, B.T.; Grunder, A.L.; Duncam, R.A.; Deino, A.L. Geochronology of age-progressive volcanism of the Oregon High Lava Plains: Implications for the plume interpretation of Yellowstone. *J. Geophys. Res.* **2004**, *109*, B10202. [CrossRef]
40. MacLeod, N.S.; Walker, G.W.; McKee, E.H. *Geothermal Significance of Eastward Increase in Age of Upper Cenozoic Rhyolitic Domes in Southeastern Oregon*; U.S. Geological Survey Open-File Report 75-034, 1-21; Geological Society of America: Boulder, CO, USA, 1975.
41. Geist, D.; Richards, M. Origin of the Columbia Plateau and Snake River plain: Deflection of the Yellowstone plume. *Geology* **1993**, *21*, 789–792. [CrossRef]
42. Christiansen, E.H.; McCurry, M. Contrasting origins of Cenozoic silicic volcanic rocks from the western Cordillera of the United States. *Bull. Volcanol.* **2008**, *70*, 251–267. [CrossRef]
43. Rytuba, J.J.; Vander Meulen, D.B. Hot-spring precious-metal systems in the Lake Owyhee volcanic field, Oregon-Idaho. In *Geology and Ore Deposits of the Great Basin: Geological Society of Nevada Symposium Proceedings*; Raines, G., Lisle, R.E., Schafer, R.W., Wilkinson, W.H., Eds.; Geological Society of America: Boulder, CO, USA, 1991; Volume 2, pp. 1085–1096.
44. Walker, G.W. Revisions to the Cenozoic stratigraphy of Harney Basin, southeastern Oregon. *U.S. Geol. Surv. Bull.* **1979**, *1475*, 41.
45. Noble, D.C.; Henry, C.D.; Park, S.L.; Smith, J.A.; Hausback, B.P.; Hilton, R.P. Geologic framework and evolution of the High Rock Canyon volcanic center, northwestern Nevada: An early caldera-focused system of the Yellowstone hotspot track. *GSA Abstr. Programs* **2009**, *41*, 57.
46. Wypych, A.; Hart, W.; Scarberry, K.; McHugh, K.; Pasquale, S.A.; Legge, P.W. *Geologic Map of the Hawks Valley–Lone Mountain Region, Harney County, Oregon*; Oregon Department of Geology and Mineral Industries Open-File Report 0–11–12; Oregon Department of Geology and Mineral Industries: Portland, OR, USA, 2011; 28p.
47. Eagar, K.C.; Fouch, M.J.; James, D.E.; Carlson, R.W. Crustal structure beneath the High Lava Plains of eastern Oregon and surrounding regions from receiver function analysis. *J. Geophys. Res.* **2011**, *116*, B02313. [CrossRef]
48. Obrebski, M.; Allen, R.M.; Xue, M.; Hung, S.-H. Slab-plume interaction beneath the Pacific Northwest. *Geophys. Res. Lett.* **2010**, *37*, LI4305. [CrossRef]
49. Shervais, J.W.; Hanan, B.B. Lithospheric topography, tilted plumes, and the track of the Snake River-Yellowstone hot spot. *Tectonics* **2008**, *27*, 2181. [CrossRef]
50. Camp, V.E.; Wells, R.E. The Case for a Long-Lived and Robust Yellowstone Hotspot. *GSA Today* **2020**, *31*, 4–10. [CrossRef]
51. Wells, R.; Bukry, D.; Friedman, R.; Pyle, D.; Duncan, R.; Haeussler, P.; Wooden, J. Geologic history of Siletzia, a large igneous province in the Oregon and Washington Coast Range: Correlation to the geomagnetic polarity time scale and implications for a long-lived Yellowstone hotspot. *Geosphere* **2014**, *10*, 692–719. [CrossRef]
52. Stern, R.J.; Dumitru, T.A. Eocene initiation of the Cascadia subduction zone: A second example of plume-induced subduction initiation? *Geosphere* **2019**, *15*, 659–681. [CrossRef]
53. Johnston, S.T.; Thorkelson, D.J. Continental flood basalts: Episodic magmatism above long-lived hotspots. *Earth Planet Sci. Lett.* **2000**, *175*, 247–256. [CrossRef]
54. Large, A.M. Silicic volcanism at the northern and western extent of the Columbia River Basalt rhyolite flare-up: Rhyolites of Buchanan volcanic complex and Dooley Mountain volcanic complex, Oregon. Master's Thesis, Portland State University, Portland, OR, USA, 2016; 190p. [CrossRef]
55. Evans, G. *Geologic Map of the Dooley Mounntain Quadrangle, Baker County, Oregon*; US Geol Surv Geologic Quadrangle Ma GQ-1694; U.S. Geological Survey: Baltimore, MD, USA, 1992.
56. Robyn, T.L. Geology and petrology of the Strawberry Mountain volcanic series, Central Oregon. Ph.D. Thesis, University of Oregon, Eugene, OR, USA, 1977.
57. Steiner, A.; Streck, M.J. *The Strawberry Volcanics: Generation of 'Orogenic' Andesites from Tholeiite within an Intra-Continental Volcanic Suite Centered on the Columbia River Flood Basalt Province, in Orogenic Andesites and Crustal Growth*; Gómez-Tuena, A., Straub, S.M., Zellmer, G.F., Eds.; Geological Society, London, Special Publications: London, UK, 2013; Volume 385. [CrossRef]
58. Dvorak, C.L.; Streck, M.J. *Geologic Map of the Jump Off Joe Mountain Quadrangle, Oregon: U.S. Geological Survey EdMap, Scale 1:24,000, 1 Sheet. 2019*; U.S. Geological Survey: Baltimore, MD, USA, 2019.
59. Dvorak, C.L.; Streck, M.J. *Geologic Map of the Big Canyon Quadrangle, Oregon: U.S. Geological Survey EdMap, Scale 1:24,000, 1 Sheet. 2020*; Geological Survey: Baltimore, MD, USA, 2020.
60. Cahoon, E.B.; Streck, M.J.; Ferns, M. Flood basalts, rhyolites, and subsequent volcanism of the Columbia River magmatic province in eastern Oregon, USA. In *From Terranes to Terrains: Geologic Field Guides on the Construction and Destruction of the Pacific Northwest: Geological Society of America Field Guide*; Booth, A.M., Grunder, A.L., Eds.; Geological Society of America: Boulder, CO, USA, 2021; Volume 62, pp. 301–352. [CrossRef]
61. Brown, C.E.; Thayer, T.P. *Geologic Map of the Canyon City Quadrangle, Northeastern Oregon: U.S. Geological Survey Miscellaneous Geologic Investigations Map I-447, scale 1:250,000.1967*; Geological Survey: Baltimore, MD, USA, 1967.
62. Dvorak, C.L. Distribution and Characterization of Rhyolites of the Strawberry Mountain Volcanics—Evolution of a Major rhyolite Field Associated with Columbia River Basalt Group Magmatism, Eastern Oregon, USA. Master's Thesis, Portland State University, Portland, OR, USA, 2021; 195p. [CrossRef]
63. Ford, M.T.; Grunder, A.L.; Duncan, R.A. Bimodal volcanism of the High Lava Plains and Northwestern Basin and Range of Oregon: Distribution and tectonic implications of ageprogressive rhyolites. *Geochem. Geophys. Geosyst.* **2013**, *14*, 2836–2857. [CrossRef]

64. Whalen, J.B.; Currie, K.L.; Chappell, B.W. A-type granites: Geochemical characteristics, discrimination and petrogenesis. *Contrib. Mineral. Petrol.* **1987**, *95*, 407–419. [CrossRef]
65. Reef, J.W. The Unity Reservoir Rhyodacite Tuff-Breccia and Associated Volcanic Rocks, Baker County, Oregon: Pullman. Master's Thesis, Washington State University, Washington, DC, USA, 1983. Volume 1128.
66. Greene, R.C.; Walker, G.W.; Corcoran, R.E. Geologic map of the Burns quadrangle. In *U.S. Geological Survey Miscellaneous Geologic Investigations Map I-680, Scale 1:250,000, 1 Sheet 1972*; Geological Survey: Baltimore, MD, USA, 1972.
67. Piper, A.M.; Robinson, T.W.; Park, C.F.; Jessup, L.T. *Geology and Groundwater Resources of the Harney Basin, Oregon, with a Statement on Precipitation and Tree Growth*; U.S. Geological Survey Water-Supply Paper; Geological Survey: Baltimore, MD, USA, 1939; Volume 841, 223p.
68. Wright, W.E.; Baisan, C.; Streck, M.; Wright, W.W.; Szejner, P. Dendrochronology and middle Miocene petrified oak: Modern counterparts and interpretation. *Palaeogeogr. Palaeoclimatol. Palaeoecol.* **2016**, *445*, 38–49. [CrossRef]
69. Hess, E. Strontium, lead, and oxygen isotopic signatures of mid-Miocene silicic volcanism in eastern Oregon. Unpubl. Master's Thesis, Portland State University, Portland, OR, USA, 2014; pp. 1–96.
70. Steiner, A.; Streck, M.J. Voluminous and compositionally diverse, middle Miocene Strawberry Volcanics of NE Oregon: Magmatism cogenetic with flood basalts of the Columbia River Basalt Group. In *Field Volcanology: A Tribute to the Distinguished Career of Don Swanson: Geological Society of America Special Paper*; Poland, M.P., Garcia, M.O., Camp, V.E., Grunder, A., Eds.; Geological Society of America: Boulder, CO, USA, 2018; Volume 538, pp. 41–62. [CrossRef]
71. Webb, B.M.; Streck, M.J.; McIntosh, W.C.; Ferns, M.L. The Littlefield Rhyolite and associated mafic lavas: Bimodal volcanism of the Columbia River magmatic province, with constraints on age and storage sites of Grande Ronde Basalt magmas. *Geosphere* **2018**, *15*, 60–84. [CrossRef]
72. Marcy, P. Revisiting Volcanology and Composition of Rhyolites and Associated REE Rich Mafic Clasts of the Three Fingers Caldera, SE Oregon. Master's Thesis, Portland State University, Portland, OR, USA, 2013; pp. 1–203.
73. Black, C. Rhyolite Stratigraphy along Succor Creek: Insights into the Eruptive History of the Three Fingers and Mahogany Mountain Volcanic Field. Master's Thesis, Portland State University, Portland, OR, USA, 2021; 158p.
74. Jackson, A. New perspective on prolific and voluminous rhyolite volcanism of the Mahogany Mountain Three Fingers Rhyolite Field, eastern Oregon. Master's Thesis, Portland State University, Oregon, Portland, 2021; 172p.
75. Kittleman, L.R.; Green, A.R.; Haddock, G.H.; Hagood, A.R.; Johnson, A.M.; McMurray, J.M.; Russell, R.G.; Weeden, D.A. *Geologic Map of the Owyhee Region, Malheur County, Oregon; Scale 1:125,000*; University of Oregon Museum of Natural History Bulletin: University of Oregon: Eugene, OR, USA, 1967.
76. Wood, J.D. The geology of the Castle Rock area, Grant, Harney and Malheur counties, Oregon. Master's Thesis, Portland State University, Portland, OR, USA, 1976; pp. 1–123.
77. Ferns, M.L.; Brooks, H.C.; Evans, J.G.; Cummings, M.L. Geologic map of the Vale 30′ x 60′ quadrangle, Malheur County, Oregon and Owyhee County, Idaho. In *Oregon Department of Geology and Mineral Industries Geologic Map Series GMS-77, Scale 1:100,000*; Oregon Department of Geology and Mineral Industries: Portland, OR, USA, 1993.
78. Rytuba, J.J.; Minor, S.A.; McKee, E.H. *Geology of the Whitehorse Caldera and Caldera-Fill Deposits, Malheur County, Oregon*; U.S. Geological Survey Open-File Report 811092; Geological Survey: Baltimore, MD, USA, 1981; 19p.
79. Hanna, T.R. Areal extent and volumes of the Dinner Creek Tuff units, eastern Oregon based on lithology, bulk rock composition and feldspar mineralogy. Master's Thesis, Portland State University, Portland, OR, USA, 2018; 144p. [CrossRef]
80. Cruz, M.; Streck, M.J. The Castle Rock and Ironside Mountain calderas, eastern Oregon, USA: Adjacent venting sites of two Dinner Creek Tuff units—The most widespread tuffs associated with Columbia River flood basalt volcanism. *Geol. Soc. Am. Bull.* **2022**, *134*, 2415–2435. [CrossRef]
81. Sales, H.J. The Wildcat Creek Tuff, eastern Oregon: Co-eruption of crystal-poor rhyolite and Fe-rich andesite with implication for mafic underpinnings to voluminous A-type rhyolites. Master's Thesis, Portland State University, Portland, OR, USA, 2018; 151p. [CrossRef]
82. Lees, K.R. Magmatic and Tectonic Changes through Time in the Neogene Volcanic Rocks of the Vale Area, Oregon, Northwestern USA. Ph.D. Thesis, Open University, Milton Keynes, UK, 1994; pp. 1–283.
83. Bonnichsen, B.; Kauffman, D.F. Physical features of rhyolite lava flows in the Snake. *Geol. Soc. Am. Spec. Pap.* **1987**, *212*, 119–145.
84. Branney, M.J.; Bonnichsen, B.; Andrews, G.D.M.; Ellis, B.; Barry, T.L.; McCurry, M. 'Snake River (SR)-type' volcanism at the Yellowstone hotspot track: Distinctive products from unusual, high-temperature silicic super-eruptions. *Bull. Volcanol.* **2008**, *70*, 293–314. [CrossRef]
85. Vander Meulen, D.B.; Rytuba, J.J.; Minor, S.A.; Harwood, C.S. Preliminary Geologic Map of the Three Fingers Rock quadrangle, Malheur County, Oregon. U.S. Geological Survey Open-File Report 89-344; U.S. Geological Survey: Baltimore, MD, USA, 1989.
86. Vander Meulen, D.B.; Rytuba, J.J.; Vercoutere, T.L.; Minor, S.A. Geologic Map of the Rooster Comb 7.5′ Quadrangle, Malheur County, Oregon. U.S. Geological Survey Miscellaneous Field Studies Map, MF-1902C, scale 1:24,000; U.S. Geological Survey: Baltimore, MD, USA, 1987.
87. Benson, T.R.; Mahood, G.A. Geology of the mid-Miocene Rooster Comb caldera and Lake Owyhee volcanic field, eastern Oregon: Silicic volcanism associated with Grande Ronde flood basalt. *J. Volcanol. Geotherm. Res.* **2016**, *309*, 96–117. [CrossRef]

88. Kuiper, K.F.; Deino, A.; Hilgen, F.J.; Krijgsman, W.; Renne, P.R.; Wijbrans, J.R. Synchronizing rock clocks of earth history. *Science* **2008**, *320*, 500. [CrossRef] [PubMed]
89. Feeney, D.M.; Isakson, V.H.; Lewis, R.S.; Mertzman, S.A. Mapping middle Miocene volcanic rocks in the Weiser Embayment, southwest Idaho: New U-PB Tims zircon age data. GSA abstract with programs. 2017. Available online: https://gsa.confex.com/gsa/2017AM/webprogram/Paper307041.html (accessed on 6 January 2023).
90. MacLean, J.W. Geology and Geochemistry of Juniper Ridge, Horsehead Mountain and Burns Butte: Implications for the petrogenesis of silicic magmas on the High Lava Plains, southeastern Oregon. Master's Thesis, Oregon State University, Corvallis, OR, USA, 1994; 141p.
91. John, D.A. Miocene and early Pliocene epithermal gold-silver deposits in the Great Basin, western United States: Characteristics, distribution, and relationship to magmatism. *Econ. Geol.* **2001**, *96*, 1827–1853. [CrossRef]
92. Wallace, A.R. Geology of the Ivanhoe Hg-Au district, northern Nevada: Influence of Miocene Volcanism, Lakes, and active faulting on epithermal mineralization. *Econ. Geol.* **2003**, *98*, 409–424. [CrossRef]
93. Cruz, M.A.; Streck, M.J. *Geologic Map of the Calamity Butte Quadrangle*; Oregon: U.S. Geological Survey EDMAP project; U.S. Geological Survey: Baltimore, MD, USA, 2017.
94. Isom, S.I.; Streck, M.J. Geologic Map of the Telephone Butte Quadrangle, Oregon: U.S. Geological Survey EDMAP project. 2016. Available online: https://ngmdb.usgs.gov/Prodesc/proddesc_109646.htm (accessed on 6 January 2023).
95. Mathis, A.C. Geology and Petrology of a 26-Ma trachybasalt to Peralkaline Rhyolite Suite Exposed at Hart Mountain, Oregon. Master's Thesis, Oregon State University, Corvallis, OR, USA, 1993; 141p.
96. McClaughry, J.D.; Ferns, M.L.; Streck, M.J.; Patridge, K.A.; Gordon, C.L. Paleogene calderas of central and eastern Oregon: Eruptive sources of widespread tuffs in the John Day and Clarno Formations. In *Volcanoes to Vineyards: Geologic Field Trips through the Dynamic Landscape of the Pacifi c Northwest: Geological Society of America Field Guide*; O'Connor, J.E., Dorsey, R.J., Madin, I.P., Eds.; Geological Society of America: Boulder, CO, USA, 2009; Volume 15, pp. 407–434. [CrossRef]
97. Meigs, A.; Scarberry, K.; Grunder, A.; Carlson, R.; Ford, M.T.; Fouch, M.; Grove, T.; Hart, W.K.; Iademarco, M.; Jordan, B.; et al. Geological and Geophysical Perspectives on the Magmatic and Tectonic Development, High Lava Plains and Northwest Basin and Range. In *Volcanoes to Vineyards*; Geological Society of America: Boulder, CO, USA, 2009.
98. Cahoon, E.B.; Streck, M.J.; Koppers, A.A.P. Picture Gorge Basalt: Internal stratigraphy, eruptive patterns, and its importance for understanding CRBG magmatism. *Geosphere* **2023**, *19*, 1–25, *in press*.
99. Moore, N.E.; Grunder, A.L.; Bohrson, W.A. The three-stage petrochemical evolution of the Steens Basalt (southeast Oregon, USA) compared to large igneous provinces and layered mafic intrusions. *Geosphere* **2018**, *14*, 2505–2532. [CrossRef]
100. Cahoon, E.B.; Streck, M.J.; Koppers, A.A.; Miggins, D.P. Reshuffling the Columbia River Basalt chronology—Picture Gorge Basalt, the earliest-and longest-erupting formation. *Geology* **2020**, *48*, 348–352. [CrossRef]
101. Reidel, S.P.; Tolan, T.L. The Grande Ronde Basalt, Columbia River Basalt Group. In *The Columbia River Flood Basalt Province: Geological Society of America Special Paper*; Reidel, S.P., Camp, V.E., Ross, M.E., Wolff, J.A., Martin, B.S., Tolan, T.L., Wells, R.E., Eds.; Geological Society of America: Boulder, CO, USA, 2013; Volume 497, pp. 117–153. [CrossRef]
102. Kasbohm, J.; Schoene, B. Rapid eruption of the Columbia River flood basalt and correlation with the mid-Miocene climate optimum. *Sci. Adv.* **2018**, *4*, eaat8223. [CrossRef]
103. Mahood, G.A.; Benson, T.R. Using $^{40}Ar/^{39}Ar$ ages of intercalated silicic tuffs to date flood basalts: Precise ages for Steens Basalt Member of the Columbia River Basalt Group. *Earth Planet. Sci. Lett.* **2017**, *459*, 340–351. [CrossRef]
104. Townsend, M.; Huber, C.; Degruyter, W.; Bachmann, O. Magma chamber growth during intercaldera periods: Insights from thermo-mechanical modeling with applications to Laguna del Maule, Campi Flegrei, Santorini, and Aso. *Geochem. Geophys. Geosyst.* **2019**, *20*, 1574–1591. [CrossRef]
105. Streck, M.J.; Grunder, A.L. Enrichment of basalt and mixing of dacite in the rootzone of a large rhyolite chamber: Inclusions and pumices from the Rattlesnake Tuff, Oregon. *Contrib. Miner. Pet.* **1999**, *136*, 193–212. [CrossRef]
106. Beard, J.S.; Lofgren, G.E. Dehydration melting and watersaturated melting of basaltic and andesitic greenstones and amphibolites at 1, 3, and 6.9 kb. *J. Petrol.* **1991**, *32*, 365–401. [CrossRef]
107. Leeman, W.P.; Whelan, J.F. *Oxygen and Strontium Isotopic Studies of Basaltic Lavas from the Snake River Plain, Idaho*; U.S. Geological Survey Open-File Report; Idaho Geological Survey: Moscow, ID, USA, 1983; Volume 83, 34p.
108. Leeman, W.P.; Oldow, J.S.; Hart, W.K. Lithosphere-scale thrusting in the western U.S. Cordillera as constrained by Sr and Nd isotopic transitions in Neogene volcanic rocks. *Geology* **1992**, *20*, 63–66. [CrossRef]
109. Manley, C.R.; McIntosh, W.C. The Juniper Mountain volcanic center, Owyhee County, southwestern Idaho: Age relations and physical volcanology. In *Tectonic and Magmatic Evolution of the Snake River Plain Volcanic Province: Idaho Geological Survey Bulletin*; Bonnichsen, B., McCurry, M., White, C.M., Eds.; Idaho Geological Survey: Moscow, ID, USA, 2002; Volume 30, pp. 205–277.
110. Bonnichsen, B.; McCurry, M.; Godchaux, M. Miocene Snake River Plain rhyolites of the Owyhee Front, Owyhee count, Idaho. In *Geological Field Trips in Southern Idaho, Eastern Oregon, and Northern Nevada, Boise*; Haller, K.M., Wood, S.H., Eds.; U.S.G.S Open-File report posted on the internet in 2004; Department of Geosciences, Boise State University: Boise, ID, USA, 2004; pp. 155–173.

111. Coats, R.L.; Hay, R.L.; Anderson, D.A. The Circle Creek Rhyolite, a volcanic complex in northern Elko county, Nevada. *GSA Mem.* **1968**, *116*, 69–100.
112. Nash, B.P.; Perkins, M.E.; Christensen JNLee, D.-C.; Halliday, A.N. The Yellowstone hot in space and time: Nd and Hf isotopes in silicic magmas. *Earth Planet. Sci. Lett.* **2006**, *247*, 143–156. [CrossRef]